

A SPECTRAL PALM ALGORITHM FOR MATRIX AND TENSOR-TRAIN BASED DICTIONARY LEARNING *

DOMITILLA BRANDONI[†], MARGHERITA PORCELLI^{†,‡}, AND VALERIA SIMONCINI^{†,§}

Abstract. Dictionary Learning (DL) is one of the leading sparsity promoting techniques in the context of image classification, where the “dictionary” matrix D of images and the sparse matrix X are determined so as to represent a redundant image dataset. The resulting constrained optimization problem is nonconvex and non-smooth, providing several computational challenges for its solution. To preserve multidimensional data features, various tensor DL formulations have been introduced, adding to the problem complexity. We develop a new alternating algorithm for the solution of the DL problem both in the matrix and tensor frameworks; in the latter case a new formulation based on Tensor-Train decompositions is also proposed. The new method belongs to the Proximal Alternating Linearized Minimization (PALM) algorithmic family, with the inclusion of second order information to enhance efficiency. We discuss a rigorous convergence analysis, and report on the new method performance on the image classification of several benchmark datasets.

Key words. Dictionary Learning, Tensor-Train decomposition, Nonconvex-nonsmooth minimization, Alternating minimization, Proximal gradient algorithms, Spectral gradient method

AMS subject classifications. 65F30, 15A23, 15A69, 65K05, 90C06.

1. Introduction. Sparse representation of data has become an important tool in a variety of contexts such as image classification and compression, observation denoising and equation solving. In the context of image classification, Dictionary Learning (DL) is among the leading sparsity promoting techniques, and we refer to [20] and [34] for an overview of all applications of dictionary learning in image processing in general.

Given an array of data Y , DL aims to find a matrix D called dictionary and a sparse matrix X to represent Y as $Y \approx DX$, under certain constraints on D and X . Each column of the dictionary D can be seen as a compressed representation of the redundant information contained in Y . A distinctive feature of this approximate factorization is that the number of columns of the dictionary D , called atoms, is greater than the number of rows. A rich number of atoms may have advantages in terms of invariance of the dictionary under specific geometric transformations, such as translations or rotations, so called “shiftability” [42, 45].

While originally the problem was formulated so that only X was an unknown data, the seminal works [1, 38] introduced a different perspective, where both D and X are to be determined. From a computational view point, this nonlinearity creates big challenges, especially when constraints are included. To cope with nonlinearity, most DL algorithms rely on *alternating* optimization: the minimization in X is known as *sparse coding* and it is often performed via the so called Orthogonal Matching Pursuit (OMP), while the minimization in D is known as *dictionary update* and various approaches have been proposed. The Method of Optimal Directions ([21]) computes the dictionary by setting to zero the partial gradient in D of the objective function.

*Version of March 10, 2022. The first and the third authors are members of the INdAM Research Group GNCS that partially supported this work.

[†]Dipartimento di Matematica, AM², Alma Mater Studiorum - Università di Bologna, Piazza di Porta San Donato 5, 40126 Bologna, Italia. Emails: {domitilla.brandoni2,margherita.porcelli,valeria.simoncini}@unibo.it

[‡]ISTI-CNR, Via Moruzzi 1, Pisa, Italia

[§]IMATI-CNR, Via Ferrata 5/A, Pavia, Italia

The K-SVD ([1]) updates each dictionary atom separately by using the Singular Value Decomposition to sequentially obtain a series of best rank-one approximations in each mode. To avoid the computation of several singular value decompositions, the Approximate K-SVD (AK-SVD) was proposed in [43]. An exhaustive overview of the matrix DL algorithms can be found in [20].

Due to the increased need to analyze multidimensional data, various tensor formulations of the DL problem have been introduced with the aim of preserving data structure and feature heterogeneity. For instance, Tensor SVD (tSVD), the Canonical Polyadic Decomposition (CPD) and the High Order SVD have been used, see, e.g., [19, 41, 49]. Each atom of the dictionary is updated separately using the corresponding tensor decomposition. In [51] the tensor data \mathcal{Y} is modeled using a sparse Tucker Decomposition, the sparsity is imposed on the core tensor \mathcal{X} , while the dictionary is replaced by the factor matrices in the Tucker decomposition. The decomposition is determined by an alternating iteration using a gradient descent method, where the sparse tensor \mathcal{X} is obtained using a greedy algorithm, named Tensor Orthogonal Matching Pursuit (TOMP). Another interesting and more recent tensor formulation can be found in [16] where the dictionary is represented as a sum of Kronecker products of smaller subdictionaries. This is equivalent to imposing a CP structure on the corresponding dictionary tensor. An analogous Kronecker structure was considered in [25, 44] where the authors show that, given a sufficient number of noisy training columns in Y , and under certain conditions on the problem parameters, the structured dictionary is locally identifiable with high probability.

When nonconvex and non-smooth models for the DL problem are considered, the tensor-based minimization procedures available in the literature are not usually supported by a theoretical analysis providing global convergence guarantees, thus limiting this methodology to a purely exploratory setting.

We advance the algorithmic developments by proposing a new nonconvex and non-smooth theoretically founded alternating algorithm for the matrix and tensor formulations of the DL problem. In the tensor case, we propose a novel application of the Tensor-Train (TT) decomposition leading to a multi-dimensional dictionary, called TT-DL. The new algorithm belongs to the class of proximal alternating linearized minimization (PALM) algorithms and is named spectral PALM (sPALM). The original PALM algorithm was presented in [10] and several variants were later proposed [17, 23, 28, 40] and applied to various problems, including standard matrix based DL problem formulations as shown in [3, 33, 50]. These methods, called PALM-type algorithms, perform a gradient step in each variable and take into account the constraints using proximal maps. Remarkably, convergence to critical points is ensured for these algorithms for a large class of nonconvex non-smooth problems where the variable vector is split into several blocks of variables. PALM-type algorithms are generally based on the use of Lipschitz constants that may be unavailable or hard to estimate, possibly leading to low performance. Our new method sPALM differs in the choice of the stepsize as it implicitly embeds second order information of the objective function, so as to take longer steps than using the more conservative Lipschitz-based stepsizes. As a consequence, sPALM is a PALM-type algorithm with the same convergence properties but with an expected better practical performance. The use of enriched proximal steps for solving composite optimization problems, that is problems where the objective is the sum of a smooth and a non-smooth function, is not new, see, e.g., [47] and the more recent advances using inexact variable metric in [12] and Newton-like steps in [30]. The novelty of our approach consists in constructing

spectral stepsizes that use information from the previous iteration of the alternating algorithm allowing to relate them with local second order information of the smooth part of the objective function. In particular, when sPALM is applied to DL, we provide new explicit bounds for the spectral stepsizes that generalize known results for strictly convex quadratic problems [18].

In this work we show that PALM-type algorithms (including sPALM) can be naturally applied to the proposed Tensor-Train DL formulation, yielding convergent schemes. Moreover, in the matrix and tensor setting, the proposed spectral variant yields better performance in the solution of DL image classification problems. To the best of our knowledge, these are the first globally convergent tensor-based algorithms in the DL literature.

This paper is organized as follows. In section 2 we describe the matrix DL problem and its use in image classification, and provide new formulations based of the TT decomposition of the dictionary. Then we illustrate the main algorithmic framework of this work, i.e. the PALM methods, in Section 3, and propose sPALM in Section 4 where the theoretical analysis is carried-out. The application of PALM algorithms to the proposed DL formulation is described in Section 5 where their convergence is also proved. Section 6 is devoted to numerical tests and conclusions are drawn in Section 7.

Notation. Vectors and scalars are denoted by lowercase letters (a, b, \dots), matrices are denoted by capital letters (A, B, \dots) and higher-order tensors by calligraphic letters ($\mathcal{A}, \mathcal{B}, \dots$). Capital Greek letters (e.g., Ω, Γ, Θ) indicate specific sets of real matrices. In the following, $\|\cdot\|_F$ indicates the matrix Frobenius norm, $\|A\|_2$ denotes the matrix norm induced by the Euclidean vector norm, while $\|x\|_0$ denotes the zero-norm of a vector or tensor, defined as the number of its nonzero entries.

2. The DL problem and a new tensor formulation. For a *training* set of data, Dictionary Learning consists of solving a two variable optimization problem. We are interested in the following formulation: Given the array $Y = [y_1, \dots, y_p] \in \mathbb{R}^{n \times p}$ and a sparsity threshold $\tau > 0$, solve

$$\min_{D, X} \|Y - DX\|_F^2 \quad s.t. \quad D \in \Omega_{n,k}, \quad X \in \Gamma_{k,p}^{(\tau)}, \quad (2.1)$$

where $k > n$ and

$$\Omega_{n,k} = \{D = [d_1, \dots, d_k] \in \mathbb{R}^{n \times k} : \|d_i\|_2 = 1, i = 1, \dots, k\} \quad (2.2)$$

$$\Gamma_{k,p}^{(\tau)} = \{X = [x_1, \dots, x_p] \in \mathbb{R}^{k \times p} : \|x_i\|_0 \leq \tau, i = 1, \dots, p\}. \quad (2.3)$$

Other formulations, not necessarily equivalent, are possible [3, 22, 34]. This minimization problem is NP-hard, see e.g. [20, 34], and nonconvex. Nonconvexity comes from two sources: the sparsity promoting functional l_0 -norm and the bi-linearity between the dictionary D and the sparse representation X . In addition, the l_0 -norm makes the problem non-smooth.

To preserve the multidimensional structure of the data, a more general *tensor* form of the DL problem can also be used. More precisely, consider for instance a fourth-dimensional array $\mathcal{Y} \in \mathbb{R}^{n_1 \times n_2 \times n_e \times n_p}$ consisting of $n_1 \times n_2$ images of n_p persons in n_e expressions. Using the $\binom{m}{n}$ -mode product (see this and related definitions in Appendix B) and the constraint sets defined in (2.2) and (2.3), the tensor DL problem can be formulated as

$$\min_{\mathcal{D}, \mathcal{X}} \|\mathcal{Y} - \mathcal{D} \times_3^1 \mathcal{X}\|_F^2 \quad s.t. \quad \mathcal{D}_{[2]} \in \Omega_{n_1 n_2, k}, \quad \mathcal{X}_{[1]} \in \Gamma_{k, n_e n_p}^{(\tau)}, \quad (2.4)$$

where $\mathcal{D} \in \mathbb{R}^{n_1 \times n_2 \times k}$ is a third-order tensor with unit norm frontal slices, and $\mathcal{X} \in \mathbb{R}^{k \times n_e \times n_p}$ is a sparse tensor with at most τ nonzero elements per column fiber, and $k > n_1 n_2$. All the constraints proper of the matrix setting can be reformulated on the tensors themselves or on their matricizations. The formulation (2.4) is equivalent to (2.1) since $\|\mathcal{Y} - \mathcal{D} \times_3^1 \mathcal{X}\|_F = \|(\mathcal{Y} - \mathcal{D} \times_3^1 \mathcal{X})_{[2]}\|_F = \|\mathcal{Y}_{[2]} - \mathcal{D}_{[2]} \mathcal{X}_{[1]}\|_F$. To reduce memory requirements, instead of considering the whole tensor \mathcal{D} , we propose its Tensor-Train (TT) Decomposition (see Definition B.4). For third order tensors the TT decomposition can be written using either the $\binom{m}{n}$ -mode product or the n -mode product (B.2) as $\mathcal{D} = G_1 \times_2^1 \mathcal{G}_2 \times_3^1 G_3 = \mathcal{G}_2 \times_1 G_1 \times_3 G_3^T$, where $G_1 \in \mathbb{R}^{n_1 \times r_1}$, $\mathcal{G}_2 \in \mathbb{R}^{r_1 \times n_2 \times r_2}$, $G_3 \in \mathbb{R}^{r_2 \times k}$ are the TT-cores and r_1, r_2 are the TT-ranks. Following the original TT-SVD algorithm, we require the columns of G_1 and of $(\mathcal{G}_2)_{[2]}$ to be orthonormal. This orthogonality property makes the computation of the Lipschitz constants more convenient (see Proposition 5.2), and the constraint on \mathcal{D} easier to handle. To properly define the Tensor-Train formulation of the DL problem the following additional constraint set of matrices with orthonormal columns is introduced,

$$\Theta_{m,n} = \{G \in \mathbb{R}^{m \times n} : G^T G = I_n\}. \quad (2.5)$$

Then, the TT formulation of the DL problem takes the form

$$\begin{aligned} \min_{G_1, \mathcal{G}_2, G_3, \mathcal{X}} \|\mathcal{Y} - (G_1 \times_2^1 \mathcal{G}_2 \times_3^1 G_3) \times_3^1 \mathcal{X}\|_F^2 \quad s.t. \quad & \mathcal{X}_{[1]} \in \Gamma_{k, n_e n_p}^{(\tau)} \quad G_1 \in \Theta_{n_1, r_1} \\ & (\mathcal{G}_2)_{[2]} \in \Theta_{r_1 n_2, r_2} \quad G_3 \in \Omega_{r_2, k} \end{aligned} \quad (2.6)$$

By tensor unfolding $\|\mathcal{Y} - (G_1 \times_2^1 \mathcal{G}_2 \times_3^1 G_3) \times_3^1 \mathcal{X}\|_F = \|\mathcal{Y}_{[2]} - (I_{n_2} \otimes G_1) (\mathcal{G}_2)_{[2]} G_3 \mathcal{X}_{[1]}\|_F$. The constraints on G_3 and $\mathcal{X}_{[1]}$ are inherited from the DL formulation. In particular, using the TT formulation, the constraint on the columns of $\mathcal{D}_{[2]}$ in (2.4) becomes a constraint on the columns of G_3 . This can be easily proved using the orthogonality of G_1 and $(\mathcal{G}_2)_{[2]}$.

The TT formulation described above can be extended to a multiway tensor $\mathcal{Y} \in \mathbb{R}^{n_1 \times \dots \times n_q \times \dots \times n_s}$ with $q < s$, as

$$\begin{aligned} \min_{G_1, \dots, G_{q+1}, \mathcal{X}} \|\mathcal{Y} - (G_1 \times_2^1 \mathcal{G}_2 \times_3^1 \dots \times_3^1 G_{q+1}) \times_{q+1}^1 \mathcal{X}\|_F^2 \quad s.t. \quad & (2.7) \\ \mathcal{X}_{[1]} \in \Gamma_{k, n_{q+1} \dots n_s}^{(\tau)}, \quad G_1 \in \Theta_{n_1, r_1} \quad G_{q+1} \in \Omega_{r_q, k}, \\ (\mathcal{G}_j)_{[2]} \in \Theta_{r_{j-1} n_j, r_{j+1}} \quad \text{for } j = 2, \dots, q. \end{aligned}$$

This formulation can be used when either the dimensionality of the database or the dimensionality of the single data is higher than 2; see, e.g., Section 6.6.

2.1. The DL classification problem. Classification is one of the major tasks within data mining; we refer the reader to [20, Chapter 8] for an overview of different DL classification algorithms. Among them, two approaches seem to be highly rated in the DL literature. In the first, the dictionary D and the sparse matrix X are learnt from data by solving (2.1) and a classifier matrix $W \in \mathbb{R}^{n_p \times k}$ is computed a posteriori as the solution of the following problem:

$$\min_W \|C - WX\|_F^2 + \beta \|W\|_F^2, \quad (2.8)$$

where β is a positive small constant, and the matrix $C \in \mathbb{R}^{n_p \times n_e n_p}$ contains the labels of the images stored in Y . In particular, if the column i of Y contains the person

ℓ , then the i th column of C is equal to e_ℓ , the ℓ th canonical basis vector. Different values of β were investigated in our computational experiments. Since this stage of the computation is not our main algorithmic concern, we will report numerical results only for $\beta = 0$.

In the second category of classification algorithms the classifier W is learnt from the data together with X and D :

$$\min_{D, X, W} \|Y - DX\|_F^2 + \gamma \|C - WX\|_F^2 \quad s.t. \quad D \in \Omega_{n,k}, \quad X \in \Gamma_{k,p}^{(\tau)}, \quad (2.9)$$

where γ is a positive constant. This formulation aims to enforce a representative strength together with a discriminative action. For this reason this classification algorithm has been named “discriminative DL”; see, e.g., [20, sec.8.5.2] and references therein. To maintain the presentation sufficiently concise, we will not further discuss this second formulation, although all results can be adapted to this setting. We refer to [13] for a more detailed presentation.

Once the classifier has been computed, the classification task proceeds as follows: Given a new image $y \in \mathbb{R}^n$ to be classified, its sparse representation $x \in \mathbb{R}^k$ is computed, e.g., by an OMP-type algorithm¹, so that y is assigned to class $\hat{\ell} = \operatorname{argmax}_i |Wx|_i$.

Preserving the multidimensional structure of the data can be extremely useful also in classification contexts. As in the previous section, the optimization problem (2.9) involving the classifier matrix can be generalized to the (multi-order) tensor setting.

3. The general PALM framework. We first review the main properties of the original PALM algorithm as a general platform for DL oriented PALM-type algorithms. Then we introduce the new spectral PALM method (hereafter sPALM) and its convergence properties. To this end, we also need to recall certain general aspects of non-smooth nonconvex optimization and to fix our assumptions.

The Proximal Alternating Linearized Minimization (PALM) algorithm [10] provides a general setting for solving non-smooth nonconvex optimization problems of the form

$$\min_{x,y} \Psi(x,y) \quad \text{with} \quad \Psi(x,y) := H(x,y) + f_1(x) + f_2(y), \quad (3.1)$$

where the functions f_1 and f_2 are extended valued (i.e., allowing the inclusion of constraints) and H is a smooth coupling function, only required to have partial Lipschitz continuous gradients $\nabla_x H$ and $\nabla_y H$ (see more precise definitions later on). This optimization problem has become a reference tool in many machine learning and image processing methodologies, see, e.g., the examples mentioned in [40]. For each block of coordinates in (3.1), PALM performs one gradient step on the smooth part, followed by a proximal step on the non-smooth part. The method belongs to the class of Gauss-Seidel proximal schemes, also known as alternating minimization schemes, and generalizes to the nonconvex non-smooth case well-known and widely used alternating algorithms [5, 6, 11, 26, 40].

¹See, e.g., <http://www.cs.technion.ac.il/~ronrubin/software.html>. In the tensor case, we derived a new tensor-train version of OMP named OMP-TT where the sparse solution is computed using the TT-cores of the dictionary without explicitly creating \mathcal{D} . For further details see [13, Chapter 7].

An important contribution to the success of PALM was the convergence proof strategy obtained in [2, 10]. This allowed the design of new convergent alternating minimization algorithms, consisting of a sequence converging to critical points of (3.1).

The PALM algorithm relies on the knowledge of the partial Lipschitz moduli of $\nabla_x H$ and $\nabla_y H$ or of some upper estimates, and was applied to sparse non-negative matrix factorizations in [10], for which partial Lipschitz moduli are explicitly available, though its practical behavior was not investigated. Inertial variants of PALM have been later proposed with the aim of accelerating the convergence of the original algorithm [23, 28, 40]. All these variants enjoy the convergence properties of the original PALM, and are based on the Lipschitz constants explicitly available for all the addressed applications. When these constants are not explicitly known, then a backtracking scheme can be employed to approximate their action [6, 7], so that convergence results still hold. Our *nonconvex-nonsmooth* setting provides significant challenges. We consider problems of the form (3.1), for which we assume that the functions H , f_1 and f_2 satisfy the following minimal assumptions set.

ASSUMPTION A

- (A1) $f_1 : \mathbb{R}^n \rightarrow (-\infty, +\infty]$ and $f_2 : \mathbb{R}^m \rightarrow (-\infty, +\infty]$ are proper and lower semi-continuous functions such that $\inf_{\mathbb{R}^n} f_1 > -\infty$ and $\inf_{\mathbb{R}^m} f_2 > -\infty$.
- (A2) $H : \mathbb{R}^{n \times m} \rightarrow \mathbb{R}$ is continuously differentiable and $\inf_{\mathbb{R}^{n \times m}} \Psi > -\infty$.
- (A3) ∇H is Lipschitz continuous on bounded subsets of $\mathbb{R}^{n \times m}$.
- (A4) The partial gradients $\nabla_x H(x, y)$ and $\nabla_y H(x, y)$ are globally Lipschitz continuous, i.e. there exist nonnegative $L'_1(y)$ and $L'_2(x)$ such that

$$\text{fixed } y, \quad \|\nabla_x H(u, y) - \nabla_x H(v, y)\|_2 \leq L'_1(y) \|u - v\|_2, \quad \forall u, v \in \mathbb{R}^n,$$

$$\text{fixed } x, \quad \|\nabla_y H(x, u) - \nabla_y H(x, v)\|_2 \leq L'_2(x) \|u - v\|_2, \quad \forall u, v \in \mathbb{R}^m.$$

- (A5) There exist $\lambda_i^+ > 0$, $i = 1, 2$ such that

$$\sup\{L_1(y^k); k \in \mathbb{N}\} \leq \lambda_1^+, \quad \sup\{L_2(x^k); k \in \mathbb{N}\} \leq \lambda_2^+. \quad (3.2)$$

We call *partial smoothness parameters* the constants $L'_1(y)$ and $L'_2(x)$ in Assumption A4. From the definition of Lipschitz continuity it follows that if a function is Lipschitz continuous with smoothness parameter L then it is also Lipschitz continuous with any $\bar{L} \geq L$. As usual, we will call *Lipschitz constant* the smallest possible smoothness parameter of a given function; for the partial gradients of the function H it will be denoted as $L_1(y)$ and $L_2(x)$.

REMARK 1. In [10] a further assumption is made to ensure that the constants $L'_1(y)$ and $L'_2(x)$ are uniformly bounded away from zero, i.e. that there exist $\lambda_i^- > 0$, $i = 1, 2$ such that

$$\inf\{L'_1(y^k); k \in \mathbb{N}\} \geq \lambda_1^-, \quad \inf\{L'_2(x^k); k \in \mathbb{N}\} \geq \lambda_2^-. \quad (3.3)$$

In our description we avoid this assumption by choosing the partial smoothness parameters L'_1 and L'_2 safely bounded away from zero, as suggested in [10, Remark 3].

The PALM algorithm with constant stepsize is reported in Algorithm 1. In there, the standard Moreau proximal mapping is employed ([6]): Given a lower and semicontinuous function $\sigma : \mathbb{R}^m \rightarrow (-\infty, \infty]$ and a scalar $t > 0$, the proximal map is defined as follows

$$\text{prox}_t^\sigma(x) = \underset{w \in \mathbb{R}^m}{\operatorname{argmin}} \left\{ \sigma(w) + \frac{t}{2} \|w - x\|^2 \right\}. \quad (3.4)$$

Algorithm 1 PALM (with constant stepsize)

- 1: **Input:** $(x_0, y_0) \in \mathbb{R}^n \times \mathbb{R}^m$, $\eta_1, \eta_2 > 1$, $\mu_1, \mu_2 > 0$
- 2: **for** $k = 0, 1, \dots$, **do**
- 3: **Update** x : Set $L_1''(y_k) = \max\{\eta_1 L_1'(y_k), \mu_1\}$ and $\bar{\alpha}_{k,1} = 1/L_1''(y_k)$ and compute

$$x_{k+1} = \text{prox}_{1/\bar{\alpha}_{k,1}}^{f_1}(x_k - \bar{\alpha}_{k,1} \nabla_x H(x_k, y_k)) \quad (3.5)$$

- 4: **Update** y : Set $L_2''(x_{k+1}) = \max\{\eta_2 L_2'(x_{k+1}), \mu_2\}$ and $\bar{\alpha}_{k,2} = 1/L_2''(x_{k+1})$ and compute

$$y_{k+1} = \text{prox}_{1/\bar{\alpha}_{k,2}}^{f_2}(y_k - \bar{\alpha}_{k,2} \nabla_y H(x_{k+1}, y_k)) \quad (3.6)$$

- 5: **end for**
-

PALM alternates the minimization on the two blocks (x, y) and makes explicit use of the smoothness parameters $L_1''(y_k)$ and $L_2''(x_k)$. When these parameters are not available, they can be approximated by using a backtracking strategy. Indeed, setting $\Psi_1(x, y) := H(x, y) + f_1(x)$ and $L_{0,1} = 1$, at each iteration $k > 1$, the procedure starts with $L_{k,1} = L_{k-1,1}$ and then $L_{k,1}$ is increased by a constant factor, typically doubled, until the following *sufficient decrease condition* is met

$$\Psi_1(x_{k+1}, y_k) \leq \Psi_1(x_k, y_k) + \langle \nabla_x H(x_k, y_k), x_{k+1} - x_k \rangle + \frac{L_{k,1}}{2} \|x_{k+1} - x_k\|_2^2. \quad (3.7)$$

Then, the stepsize $\bar{\alpha}_{k,1}$ is taken as the reciprocal of the found value (analogously for $\bar{\alpha}_{k,2}$, where we set $\Psi_2(x, y) := H(x, y) + f_2(y)$). The following theorem reports the main convergence result proved for the original PALM algorithm and successively extended to all PALM-type algorithms², see [10, 28, 23, 40].

THEOREM 3.1. *Suppose that Ψ is semi-algebraic such that Assumptions A hold. Let $\{z_k\} = \{(x_k, y_k)\}$ be a bounded sequence generated by PALM in Algorithm 1. Then the sequence $\{z_k\}$ has finite length, that is $\sum_{k=1}^{\infty} \|z_{k+1} - z_k\| < \infty$, and converges to a critical point z^* of Ψ .*

4. The spectral PALM algorithm (sPALM). Starting from the PALM framework, we propose sPALM that, for each coordinate block, employs a *spectral* gradient step in the smooth part of the operator, while maintaining a proximal step for the non-smooth part. More precisely, sPALM uses a spectral stepsize in each variable block in combination with an Armijo-type backtracking strategy ensuring the overall convergence. Spectral³ gradient methods are well-known optimization strategies for the solution of large scale unconstrained and constrained optimization problems [9, 8]. These algorithms are rather appealing for their simplicity, low-cost per iteration (gradient-type algorithms) and good practical performance due to a clever choice of the step length. The key to the success of these approaches, also known as Barzilai-Borwein methods from the pioneering work [4], lies in the explicit use of first-order information of the cost function on the one hand and, on the other hand,

²The result can be generalized to the case of a function Ψ that satisfies the so-called Kurdyka-Lojasiewicz property, as done for PALM in [10].

³The denomination “spectral” refers to the property that the steplength is related to the spectrum of the average Hessian matrix (when well-defined).

in the implicit use of second-order information embedded in the step length through a rough approximation of the cost function Hessian. While spectral gradient methods were first proposed for convex quadratic problems, they have been widely used in a large variety of more general contexts [18, 29, 35].

Spectral stepsizes have also been used in [11] in the context of *convex* constrained optimization problems. Indeed the proposed Cyclic Block Coordinate Gradient Projection algorithm in [11] makes use of spectral stepsizes when applied to non-negative matrix factorizations. However, these steps are used to determine an approximate solution of the minimization problem for each variable block, and they do not use information from the previous iteration of the alternating algorithm. To the best of our knowledge, the use of spectral stepsizes embedded in an alternating algorithm for non-convex non-smooth problems of the form (3.1) has remained so far unexplored. We contribute to fill this gap.

Classical spectral stepsizes, also known as BB stepsizes from the initials of Barzilai and Borwein, are motivated by the quasi-Newton approach, where the inverse of the Hessian matrix is replaced by a multiple of the identity matrix [4]. Consider the case of the partial Hessian $\nabla_{xx}H$ (the case of $\nabla_{yy}H$ is analogous). For a given iteration k , let $s_k = x_{k+1} - x_k$ and $g_k = \nabla_x H(x_{k+1}, y_k) - \nabla_x H(x_k, y_k)$ be the difference between two consecutive iterates and corresponding gradient values. Then $\nabla_{xx}H(x_{k+1}, y_k)$ is approximated by $\alpha_{k+1}^{-1}I$ where the positive scalar α_{k+1} is defined by either of the following BB values

$$\alpha_{k+1}^{BB1} = \operatorname{argmin}_{\alpha} \|\alpha^{-1}s_k - g_k\| \quad \text{or} \quad \alpha_{k+1}^{BB2} = \operatorname{argmin}_{\alpha} \|s_k - \alpha g_k\|$$

that is,

$$\alpha_{k+1}^{BB1} = \frac{\langle s_k, s_k \rangle}{\langle s_k, g_k \rangle} \quad \text{or} \quad \alpha_{k+1}^{BB2} = \frac{\langle s_k, g_k \rangle}{\langle g_k, g_k \rangle}. \quad (4.1)$$

A variety of different rules based on suitable adaptive combinations of α_{k+1}^{BB1} and α_{k+1}^{BB2} in (4.1) have been proposed in the literature in the solution of “single block variable” nonlinear optimization problems and it was observed experimentally that alternating the two stepsizes along iterations is beneficial for the performance, see [18, 35] and references therein. We report in Algorithm 2 a simple alternating rule based on [27] that gives the best results in our numerical experiments (see Section 6). Other rules can be equally adapted within sPALM. The inclusion of threshold values in Algorithm 2 ensures that the α ’s remain bounded. The overall sPALM scheme is reported in Algorithm 3.

REMARK 2. *Under Assumption A, conditions (4.3) and (4.5) in Algorithm 3 are satisfied in a finite number of backtracking steps. For instance, from the descent lemma, see e.g. [10, Lemma 1], for any x defined by $x = \operatorname{prox}_{1/\alpha}^{f_1}(x_k - \alpha \nabla_x H(x_k, y_k))$ we have that*

$$\Psi_1(x, y_k) \leq \Psi_1(x_k, y_k) - \frac{1}{2} \left(\frac{1}{\alpha} - L_1(y_k) \right) \|x - x_k\|_2^2,$$

and condition (4.3) is satisfied for $\alpha \leq \frac{1-\delta_1}{L_1(y_k)}$. Therefore, backtracking terminates with $\bar{\alpha}_{k,1} \geq \min \left\{ \alpha_{k,1}, \frac{\rho_1(1-\delta_1)}{L_1(y_k)} \right\} \geq \min \left\{ \alpha_{\min}, \frac{\rho_1(1-\delta_1)}{\lambda_1^+} \right\}$. Similarly for condition (4.5).

In the following we set up the theoretical tools for proving a convergence result analogous to that of Theorem 3.1 by exploiting the proof of methodology introduced

Algorithm 2 Computation of the spectral stepsize $\alpha_{k+1,i}$, $i = 1$ or $i = 2$

1: **Input:** $s_{k,i}, g_{k,i}$, $0 < \alpha_{\min} \leq \alpha_{\max}$.
2: **if** $\langle s_{k,i}, g_{k,i} \rangle > 0$ **then**
3: **if** k is odd **then**
4: $\alpha_{k+1,i} = \max \left\{ \alpha_{\min}, \min \left\{ \alpha_{k+1,i}^{BB1}, \alpha_{\max} \right\} \right\}$ with $\alpha_{k+1,i}^{BB1} = \frac{\langle s_{k,i}, s_{k,i} \rangle}{\langle s_{k,i}, g_{k,i} \rangle}$
5: **else**
6: $\alpha_{k+1,i} = \max \left\{ \alpha_{\min}, \min \left\{ \alpha_{k+1,i}^{BB2}, \alpha_{\max} \right\} \right\}$ with $\alpha_{k+1,i}^{BB2} = \frac{\langle s_{k,i}, g_{k,i} \rangle}{\langle g_{k,i}, g_{k,i} \rangle}$
7: **end if**
8: **else**
9: $\alpha_{k+1,i} = 1$
10: **end if**

Algorithm 3 sPALM

1: **Input:** $(x_0, y_0) \in \mathbb{R}^n \times \mathbb{R}^m$, $\rho_1, \delta_1, \rho_2, \delta_2 \in (0, 1)$, $0 < \alpha_{\min} \leq \alpha_{\max}$, $\alpha_{0,1}, \alpha_{0,2} \in [\alpha_{\min}, \alpha_{\max}]$.
2: **for** $k = 0, 1, \dots$, **do**
3: **Update** x : Set

$$x_{k+1} = \text{prox}_{1/\bar{\alpha}_{k,1}}^{f_1} (x_k - \bar{\alpha}_{k,1} \nabla_x H(x_k, y_k)) \quad (4.2)$$

where $\bar{\alpha}_{k,1} = \rho_1^{i_k} \alpha_{k,1}$ and i_k is the smallest nonnegative integer for which the following condition is satisfied,

$$\Psi_1(x_{k+1}, y_k) \leq \Psi_1(x_k, y_k) - \frac{\delta_1}{2\bar{\alpha}_{k,1}} \|x_{k+1} - x_k\|_2^2 \quad (4.3)$$

4: Compute $\alpha_{k+1,1} \in [\alpha_{\min}, \alpha_{\max}]$ using Algorithm 2 with $s_{k,1} = x_{k+1} - x_k$ and $g_{k,1} = \nabla_x H(x_{k+1}, y_k) - \nabla_x H(x_k, y_k)$.
5: **Update** y : Set

$$y_{k+1} = \text{prox}_{1/\bar{\alpha}_{k,2}}^{f_2} (y_k - \bar{\alpha}_{k,2} \nabla_y H(x_{k+1}, y_k)) \quad (4.4)$$

where $\bar{\alpha}_{k,2} = \rho_2^{j_k} \alpha_{k,2}$ and j_k is the smallest nonnegative integer for which the following condition is satisfied,

$$\Psi_2(x_{k+1}, y_{k+1}) \leq \Psi_2(x_{k+1}, y_k) - \frac{\delta_2}{2\bar{\alpha}_{k,2}} \|y_{k+1} - y_k\|_2^2 \quad (4.5)$$

6: Compute $\alpha_{k+1,2} \in [\alpha_{\min}, \alpha_{\max}]$ using Algorithm 2 with $s_{k,2} = y_{k+1} - y_k$ and $g_{k,2} = \nabla_y H(x_{k+1}, y_{k+1}) - \nabla_y H(x_{k+1}, y_k)$.
7: **end for**

in [10] (see also [40, Section 3]). Standard notation and definitions of non-smooth analysis will be used, see, e.g., [36]. The convergence of sPALM is then a consequence of the convergence analysis carried out in [10] and relies on the following lemma.

LEMMA 4.1. *Suppose Assumption A holds. Let $\{z_k\} = \{(x_k, y_k)\}$ be a bounded sequence generated by sPALM from a starting point z_0 and let $\omega(z_0)$ be the set of all*

limit points of $\{z_k\}$. Then the following conditions hold.

- C1)** There exists a positive scalar γ_1 such that $\gamma_1 \|z_{k+1} - z_k\|_2^2 \leq \Psi(z_k) - \Psi(z_{k+1})$;
- C2)** There exists a positive scalar γ_2 such that for some $w_k \in \partial\Psi(z_k)$ we have $\|w_k\|_2 \leq \gamma_2 \|z_k - z_{k-1}\|$, for $k = 0, 1, \dots$;
- C3)** Each limit point in the set $\omega(z_0)$ is a critical point for Ψ .

Proof. We first observe that the stepsizes $\bar{\alpha}_{k,1}$ and $\bar{\alpha}_{k,2}$ remain bounded for all k . Indeed, since $\alpha_{k,1} \in [\alpha_{\min}, \alpha_{\max}]$ we have that $\bar{\alpha}_{k,1} = \rho_1^{i_k} \alpha_{k,1} \leq \alpha_{\max}$ as $\rho_1 \in (0, 1)$ and $i_k \geq 0$. Moreover, $\bar{\alpha}_{k,1}$ and $\bar{\alpha}_{k,2}$ are uniformly bounded from below, see Remark 2.

Item C1) can be proved as follows. Fix $k \geq 0$ and sum the inequalities (4.3) and (4.5), so as to obtain

$$\begin{aligned} \Psi_1(x_{k+1}, y_k) + \Psi_2(x_{k+1}, y_{k+1}) &\leq \Psi_1(x_k, y_k) + \Psi_2(x_{k+1}, y_k) \\ &\quad - \frac{\delta_1}{2\bar{\alpha}_{k,1}} \|x_{k+1} - x_k\|_2^2 - \frac{\delta_2}{2\bar{\alpha}_{k,2}} \|y_{k+1} - y_k\|_2^2. \end{aligned}$$

Recalling the definition of Ψ_1 and Ψ_2 around (3.7) we obtain

$$\begin{aligned} \Psi(x_{k+1}, y_{k+1}) &\leq \Psi(x_k, y_k) - \frac{\delta_1}{2\bar{\alpha}_{k,1}} \|x_{k+1} - x_k\|_2^2 - \frac{\delta_2}{2\bar{\alpha}_{k,2}} \|y_{k+1} - y_k\|_2^2 \\ &\leq \Psi(x_k, y_k) - \frac{\delta_1}{2\alpha_{\max}} \|x_{k+1} - x_k\|_2^2 - \frac{\delta_2}{2\alpha_{\max}} \|y_{k+1} - y_k\|_2^2, \end{aligned}$$

from which Item C1) follows, with $\gamma_1 = \frac{1}{2\alpha_{\max}} \min\{\delta_1, \delta_2\}$.

The proofs of items C2) and C3) follow the lines of the proofs of [10, Lemmas 4 and 5]. Indeed, from the definition of the proximal map and the iterative steps (4.2) and (4.4), we have that

$$x_k = \operatorname{argmin}_{x \in \mathbb{R}^n} \left\{ \langle \nabla_x H(x_{k-1}, y_{k-1}), x - x_{k-1} \rangle + \frac{1}{2\bar{\alpha}_{k,1}} \|x - x_{k-1}\|_2^2 + f_1(x) \right\}$$

and

$$y_k = \operatorname{argmin}_{y \in \mathbb{R}^m} \left\{ \langle \nabla_y H(x_k, y_{k-1}), y - y_{k-1} \rangle + \frac{1}{2\bar{\alpha}_{k,2}} \|y - y_{k-1}\|_2^2 + f_2(y) \right\}.$$

Using the fact that $\bar{\alpha}_{k,1}$ and $\bar{\alpha}_{k,2}$ are bounded for all k the results follow. \square

We can now state a convergence result for sPALM.

THEOREM 4.2. *Suppose that Ψ is semi-algebraic such that Assumption A holds. Let $\{z_k\} = \{(x_k, y_k)\}$ be a bounded sequence generated by sPALM. Then the sequence $\{z_k\}$ has finite length and converges to a critical point z^* of Ψ .*

Proof. The proof follows by using Lemma 4.1 and applying the proof methodology proposed in [10]. \square

REMARK 3. *Algorithm 1 and Algorithms 2-3 can be extended to the general setting involving $p > 2$ blocks, that is problems of the form*

$$\min_{x_i \in \mathbb{R}^{n_i}} \Psi(x_1, \dots, x_p) := H(x_1, \dots, x_p) + \sum_{i=1}^p f_i(x_i), \quad (4.6)$$

for which Theorems 3.1 and 4.2 hold. When variable blocks are matrices, all PALM-type algorithms can be extended to the matrix optimization setting by using the trace matrix scalar product and the Frobenius norm in place of the vector scalar product and the vector 2-norm, respectively.

5. Application of the PALM framework to DL. The PALM methodology can be applied to the DL problem in the matrix setting; see, e.g., [3, 50, 33]. We provide a general framework for DL leading to convergent schemes, that can also be employed in the case of the tensor formulation.

In the matrix case, problem (2.1) can be equivalently formulated as

$$\min_{D, X} \|Y - DX\|_F^2 + \delta_{\Omega_{n,k}}(D) + \delta_{\Gamma_{k,p}^{(\tau)}}(X), \quad (5.1)$$

where $\delta_{\Omega_{n,k}}$ and $\delta_{\Gamma_{k,p}^{(\tau)}}$ are indicator functions over the sets $\Omega_{n,k}$ and $\Gamma_{k,p}^{(\tau)}$ defined in (2.2) and (2.3), respectively. Given a non-empty and closed set $\Omega \subseteq \mathbb{R}^{m \times n}$, we recall that the indicator function $\delta_{\Omega} : \mathbb{R}^{m \times n} \rightarrow (-\infty, +\infty]$ is given by

$$\delta_{\Omega}(A) = \begin{cases} 0 & \text{if } A \in \Omega \\ +\infty & \text{otherwise.} \end{cases} \quad (5.2)$$

The formulation (3.1) has clearly the form (5.1) with $H(D, X) = \|Y - DX\|_F^2$, $f_1(D) = \delta_{\Omega_{n,k}}(D)$ and $f_2(X) = \delta_{\Gamma_{k,p}^{(\tau)}}(X)$. For these functions, it has been proved in [3, 33] that Assumptions A1-A4 hold and that the Lipschitz moduli for the partial gradients $\nabla_X H$ and $\nabla_D H$ are given, respectively, by

$$L_X = 2\|D^T D\|_2 \quad \text{and} \quad L_D = 2\|X X^T\|_2. \quad (5.3)$$

The overall objective function is semi-algebraic: H is a real polynomial function, while f_1 and f_2 are indicator functions of semi-algebraic sets, and thus semi-algebraic as well. Assuming that the sequence of iterates generated by PALM is bounded and being H twice continuously differentiable, PALM is thus guaranteed to converge to a critical point of problem (5.1), see Theorem 3.1. The same argument can be applied to sPALM invoking Theorem 4.2, and to the other PALM variants. We next give the explicit form of the BB stepsizes, where (X_k, D_k) play the role of (x_k, y_k) in Algorithms 2-3, and show some key bounds.

PROPOSITION 5.1. *Let $S_k = X_{k+1} - X_k$ and $T_k = D_{k+1} - D_k$ be computed at the k th iteration of sPALM applied to problem (5.1). Assume that $\langle S_k, (D_k^T D_k) S_k \rangle \neq 0$ and $\langle T_k, T_k (X_{k+1} X_{k+1}^T) \rangle \neq 0$. Then the BB stepsizes take the form*

$$\alpha_{X_{k+1}}^{BB1} = \frac{1}{2} \frac{\langle S_k, S_k \rangle}{\langle S_k, (D_k^T D_k) S_k \rangle} \quad \text{and} \quad \alpha_{X_{k+1}}^{BB2} = \frac{1}{2} \frac{\langle S_k, (D_k^T D_k) S_k \rangle}{\langle (D_k^T D_k) S_k, (D_k^T D_k) S_k \rangle},$$

$$\alpha_{D_{k+1}}^{BB1} = \frac{1}{2} \frac{\langle T_k, T_k \rangle}{\langle T_k, T_k (X_{k+1} X_{k+1}^T) \rangle} \quad \text{and} \quad \alpha_{D_{k+1}}^{BB2} = \frac{1}{2} \frac{\langle T_k, T_k (X_{k+1} X_{k+1}^T) \rangle}{\langle T_k (X_{k+1} X_{k+1}^T), T_k (X_{k+1} X_{k+1}^T) \rangle},$$

and the following bounds hold

$$\frac{1}{L_{X_k}} \leq \alpha_{X_{k+1}}^{BB2} \leq \min \left\{ \alpha_{X_{k+1}}^{BB1}, \frac{1}{2\sigma_{\min}^2(D_k)} \right\}$$

and

$$\frac{1}{L_{D_{k+1}}} \leq \alpha_{D_{k+1}}^{BB2} \leq \min \left\{ \alpha_{D_{k+1}}^{BB1}, \frac{1}{2\sigma_{\min}^2(X_{k+1})} \right\} \quad (5.4)$$

where $\sigma_{\min}(D_k)$ and $\sigma_{\min}(X_{k+1})$ are the smallest nonzero singular values of D_k and X_{k+1} , respectively, and L_{D_k} and $L_{X_{k+1}}$ are given in (5.3).

Proof. From the definitions of $\alpha_{X_{k+1}}^{BB1}$ and $\alpha_{X_{k+1}}^{BB2}$ in (4.1) and from observing that $\nabla_X H = -2D^T(Y - DX)$ and $\nabla_D H = -2(Y - DX)X^T$, we get the form of the BB stepsizes $\alpha_{X_{k+1}}^{BB1}$, $\alpha_{X_{k+1}}^{BB2}$, $\alpha_{D_{k+1}}^{BB1}$ and $\alpha_{D_{k+1}}^{BB2}$. Moreover, the partial Hessians of H have the form $\nabla_{XX} H = I \otimes 2(D^T D)$, $\nabla_{DD} H = 2(XX^T) \otimes I$ and are positive semidefinite. Therefore the 2-norm Lipschitz constants are $L_X = \lambda_{\max}(\nabla_{XX} H)$ and $L_D = \lambda_{\max}(\nabla_{DD} H)$.

Let us consider the stepsizes $\alpha_{X_{k+1}}^{BB1}$ and $\alpha_{X_{k+1}}^{BB2}$. We observe that they are the reciprocal of Rayleigh quotients for $2(D_k^T D_k)$ and $2(D_k D_k^T)$, using S_k and $D_k S_k$, respectively, as $\alpha_{X_{k+1}}^{BB2} = \frac{1}{2} \|D_k S_k\|_F^2 / \langle D_k S_k, (D_k D_k^T)(D_k S_k) \rangle$. Moreover,

$$\begin{aligned} \alpha_{X_{k+1}}^{BB2} &= \frac{1}{2} \frac{\langle S_k, S_k \rangle \langle S_k, (D_k^T D_k) S_k \rangle^2}{\langle S_k, (D_k^T D_k) S_k \rangle \langle (D_k^T D_k) S_k, (D_k^T D_k) S_k \rangle \langle S_k, S_k \rangle} \\ &= \alpha_{X_{k+1}}^{BB1} \frac{\|S_k\|_F^2 \|(D_k^T D_k) S_k\|_F^2 \cos^2 \phi_k}{\|S_k\|_F^2 \|(D_k^T D_k) S_k\|_F^2} = \alpha_{X_{k+1}}^{BB1} \cos^2 \phi_k \end{aligned}$$

where ϕ_k is the angle between the vectorization \hat{s}_k of S_k and $(I \otimes (D_k^T D_k)) \hat{s}_k$. Therefore,

$$\alpha_{X_{k+1}}^{BB1} \geq \alpha_{X_{k+1}}^{BB2} \geq \frac{1}{\lambda_{\max}(2(D_k^T D_k))} = \frac{1}{L_{X_k}}.$$

Finally, let $D_k = D_k^T D_k \geq 0$. Then $\alpha_{X_{k+1}}^{BB2} = \frac{1}{2} \|D_k^{\frac{1}{2}} S_k\|_F^2 / \|(D_k^{\frac{1}{2}}) D_k^{\frac{1}{2}} S_k\|_F^2 \leq 1 / (2\sigma_{\min}^2(D_k))$, where the last inequality follows from the fact that $D_k^{\frac{1}{2}} S_k$ belongs to the range of D_k .

The inequalities for $\alpha_{D_{k+1}}^{BB1}$ and $\alpha_{D_{k+1}}^{BB2}$ in (5.4) can be derived analogously. \square

Proposition 5.1 gives bounds on the BB stepsizes for the case of semidefinite Hessian and shows that longer steps are made than with the reciprocal of the Lipschitz constants. These bounds generalize to the singular case known bounds for strictly quadratic functions, see, e.g., [18]. In the strictly convex quadratic case the BB stepsizes are able to sweep the spectrum of the Hessian matrix yielding faster convergence than using a standard steepest-descent method. An analogous faster convergence is expected in practice in the (only) convex case.

Similarly, this approach can be applied to the classification problem (2.9), see [13].

We next illustrate the main contribution of this section by showing the application of the PALM framework to the tensor formulation (2.6), which can be rewritten as

$$\min_{G_1, G_2, G_3, \mathcal{X}} H(G_1, G_2, G_3, \mathcal{X}) + \delta_{\Gamma_{k, n_e n_p}^{(\tau)}}(\mathcal{X}_{[1]}) + \delta_{\Theta_{n_1, r_1}}(G_1) + \delta_{\Theta_{r_1 n_2, r_2}}((G_2)_{[2]}) + \delta_{\Omega_{r_2, k}}(G_3), \quad (5.5)$$

where $H(G_1, G_2, G_3, \mathcal{X}) = \|\mathcal{Y} - (G_1 \times_2 G_2 \times_3 G_3) \times_3 \mathcal{X}\|_F^2$. We determine explicit values⁴ for the Lipschitz constants of the partial gradient of H in (5.5), where L_S is the Lipschitz constant of H corresponding to the variable S in the $\|\cdot\|_2$ norm.

PROPOSITION 5.2. *Set $G_2 = (G_2)_{[2]}$, $X = \mathcal{X}_{[1]}$, $Y = \mathcal{Y}_{[2]}$ and consider*

$$H(G_1, G_2, G_3, X) = \|Y - (I_{n_2} \otimes G_1) G_2 G_3 X\|_F^2.$$

⁴If G_1, G_2 did not have orthonormal columns, upper bounds for the Lipschitz constants could still be obtained.

Then the partial gradients of H are globally Lipschitz. For G_1, G_2 having orthonormal columns, the Lipschitz constants satisfy

$$L_X = 2\|G_3\|_2^2, \quad L_{G_2} = 2\|G_3X\|_2^2, \quad L_{G_3} = 2\|X\|_2^2,$$

and $L_{G_1} = 2\|\sum_{i=1}^p (A_i A_i^T)\|_2$, where $A_i \in \mathbb{R}^{r_1 \times n_2}$ is the matricization of the i th column of $A = G_2 G_3 X$.

Proof. By direct computation the following expressions for the partial gradients of H hold:

$$\begin{aligned} \nabla_X H &= 2 \left((I_{n_2} \otimes G_1) G_2 G_3 \right)^T (-Y + (I_{n_2} \otimes G_1) G_2 G_3 X) \\ \nabla_{G_1} H &= 2 \sum_{i=1}^p (Y_i + G_1 A_i) A_i^T \\ \nabla_{G_2} H &= 2 (I_{n_2} \otimes G_1)^T (-Y + (I_{n_2} \otimes G_1) G_2 G_3 X) (G_3 X)^T \\ \nabla_{G_3} H &= 2 G_2^T (I_{n_2} \otimes G_1)^T (-Y + (I_{n_2} \otimes G_1) G_2 G_3 X) X^T \end{aligned}$$

where $A_i \in \mathbb{R}^{r_1 \times n_2}$ and $Y_i \in \mathbb{R}^{n_1 \times n_2}$ are the matricization of the i th column of $A = G_2 G_3 X$ and Y , respectively.

Using these expressions we show that each partial gradient is globally Lipschitz. In doing so, we derive Lipschitz constants by exploiting the orthonormality of the columns of G_1 and G_2 . For any \hat{X} and \tilde{X} we get

$$\begin{aligned} &\|\nabla_X H(G_1, G_2, G_3, \hat{X}) - \nabla_X H(G_1, G_2, G_3, \tilde{X})\|_2 \\ &= 2\|G_3^T G_2^T (I_{n_2} \otimes G_1)^T (I_{n_2} \otimes G_1) G_2 G_3 (\hat{X} - \tilde{X})\|_2 \\ &= 2\|G_3^T G_3 (\hat{X} - \tilde{X})\|_2 \leq L_X \|\hat{X} - \tilde{X}\|_2, \end{aligned} \tag{5.6}$$

with $L_X = 2\|G_3^T G_3\|_2 = 2\|G_3\|_2^2$. In a similar manner we obtain the following inequalities for $\nabla_{G_i} H$, $i = 1, 2, 3$.

In particular, for any \hat{G}_1 and \tilde{G}_1 we get

$$\begin{aligned} &\|\nabla_{G_1} H(\hat{G}_1, G_2, G_3, X) - \nabla_{G_1} H(\tilde{G}_1, G_2, G_3, X)\|_2 \\ &= 2\left\| \sum_{i=1}^p (\hat{G}_1 - \tilde{G}_1) A_i A_i^T \right\| \leq L_{G_1} \|\hat{G}_1 - \tilde{G}_1\|, \end{aligned}$$

with $L_{G_1} = 2\|\sum_{i=1}^p A_i A_i^T\|_2$. Moreover, for any \hat{G}_2 and \tilde{G}_2 , we have

$$\begin{aligned} &\|\nabla_{G_2} H(G_1, \hat{G}_2, G_3, X) - \nabla_{G_2} H(G_1, \tilde{G}_2, G_3, X)\|_2 \\ &= 2\|(I_{n_2} \otimes G_1)^T (I_{n_2} \otimes G_1) (\hat{G}_2 - \tilde{G}_2) G_3 X (G_3 X)^T\|_2 \\ &= 2\|(\hat{G}_2 - \tilde{G}_2) G_3 X (G_3 X)^T\|_2 \leq L_{G_2} \|\hat{G}_2 - \tilde{G}_2\|_2, \end{aligned} \tag{5.7}$$

where $L_{G_2} = 2\|G_3 X X^T G_3^T\|_2 = 2\|G_3 X\|_2^2$. Finally, for any \hat{G}_3 and \tilde{G}_3 we have

$$\begin{aligned} &\|\nabla_{G_3} H(G_1, G_2, \hat{G}_3, X) - \nabla_{G_3} H(G_1, G_2, \tilde{G}_3, X)\|_2 \\ &= 2\left\| G_2^T (I_{n_2} \otimes G_1)^T (I_{n_2} \otimes G_1) G_2 (\hat{G}_3 - \tilde{G}_3) X X^T \right\|_2 \\ &= 2\|(\hat{G}_3 - \tilde{G}_3) X X^T\|_2 \leq L_{G_3} \|\hat{G}_3 - \tilde{G}_3\|_2, \end{aligned}$$

where $L_{G_3} = 2\|X X^T\|_2 = 2\|X\|_2^2$. \square

As an implementation remark, we observe that the computation of the partial gradients can avoid the explicit calculation of the Kronecker product $I \otimes G_1$. Indeed, using the orthogonality of $I \otimes G_1$ and the properties of the Kronecker product, the partial gradient $\nabla_X H$ in Proposition 5.2 above can be computed as $\nabla_X H = G_3^T G_2^T (-\tilde{G}^T + G_2 G_3 X)$, where $\tilde{G} = \text{reshape}(G_1' \text{reshape}(Y, [n_1, n_2 p]), [r_1 n_2, p])$. The same applies to all the partial gradients in Proposition 5.2.

Since PALM-type algorithms at each iteration require the computation of a proximal step in each variable block, we now give the formal expression of proximal operators for the three indicator functions in (5.5). We recall that the proximal map of an indicator function δ_Ω over a non-empty and closed set $\Omega \subseteq \mathbb{R}^{m \times n}$ is the multi-valued projection $P_\Omega : \mathbb{R}^{m \times n} \rightrightarrows \Omega$ such that

$$P_\Omega(A) = \underset{B \in \Omega}{\text{argmin}} \|A - B\|_F. \quad (5.8)$$

Notice that if Ω is a convex set the projection map is single-valued. The following proposition gives a closed form expression for the corresponding projection operators over the sets $\Theta_{m,n}$, $\Omega_{m,n}$ and $\Gamma_{m,n}^{(\tau)}$.

PROPOSITION 5.3. *Let $A \in \mathbb{R}^{m \times n}$.*

- i. *Let $\Theta_{m,n} \subseteq \mathbb{R}^{m \times n}$ be defined in (2.5). Then $P_{\Theta_{m,n}}(A) = UV^T$, where U and V are respectively the left and right singular matrices of A .*
- ii. *Let $\Omega_{m,n} \subseteq \mathbb{R}^{m \times n}$ be defined in (2.2). Then $P_{\Omega_{m,n}}(A) = AS^{-1}$, where $S \in \mathbb{R}^{n \times n}$ is a diagonal matrix whose diagonal elements are the norm of the columns of A .*
- iii. *Let $\Gamma_{m,n} \subseteq \mathbb{R}^{m \times n}$ be defined in (2.3). Then $P_{\Gamma_{m,n}}(A) = \text{hard}_\tau(A)$, where hard_τ is the hard-thresholding function that selects the τ largest elements (in absolute value) of each column of A and zeroes all the others.*

Proof. For $B \in \Omega \subset \mathbb{R}^{m \times n}$ having unit norm columns, we have that $\|A - B\|_F^2 = \text{trace}(A^T A) - 2\text{trace}(B^T A) + n$ and thus solving (5.8) is equivalent to finding $B = \underset{B \in \Omega}{\text{argmax}} \text{trace}(A^T B)$.

- i) For $\Omega = \Theta_{m,n}$, let $A = U\Sigma V^T$ be the SVD of A , and let $\bar{n} = \min\{m, n\}$. Then

$$\text{trace}(B^T A) = \text{trace}(B^T U \Sigma V^T) = \text{trace}(V^T B^T U \Sigma) = \sum_{i=1}^{\bar{n}} z_{ii} \sigma_i \leq \sum_{i=1}^{\bar{n}} \sigma_i,$$

where z_{ii} is the i th diagonal element of $Z = V^T B^T U$ and σ_i are the singular values of A . In particular, note that $z_{ii} \leq 1$ as $e_i^T V^T B^T U e_i \leq \|V e_i\| \|B\| \|U e_i\| = 1$. The upper bound is reached for Z equal to the identity matrix, which is obtained for $B = UV^T$.

- ii) For $\Omega = \Omega_{m,n}$ and $A = [a_1, \dots, a_n]$, $B = [b_1, \dots, b_n]$ with $\|b_j\| = 1$, $j = 1, \dots, n$, it holds that

$$\text{trace}(B^T A) = \sum_{j=1}^n b_j^T a_j = \sum_{j=1}^n \cos(\theta_j) \|a_j\|_2 \leq \sum_{j=1}^n \|a_j\|_2,$$

where $\theta_j \in [0, \frac{\pi}{2}]$, and the upper bound is reached for $b_j = a_j / \|a_j\|_2$.

- iii) The statement follows from [10, Section 4]. \square

Algorithm 4 describes the general PALM scheme with constant stepsize applied to the tensor formulation (5.5), that is therefore named PALM-DL-TT. The Lipschitz moduli L_X, L_{G_i} $i = 1, 2, 3$ are as introduced in Proposition 5.2. This algorithm will be a reference competitor for our new method in the reported numerical experiments.

Algorithm 4 PALM-DL-TT

- 1: **Input:** Data matrix $\mathcal{Y} \in \mathbb{R}^{n_1 \times n_2 \times n_3 \times n_e \times n_p}$, initial values for $G_1 \in \mathbb{R}^{n_1 \times r_1}$, $\mathcal{G}_2 \in \mathbb{R}^{r_1 \times n_2 \times r_2}$, $G_3 \in \mathbb{R}^{r_2 \times k}$ and $\mathcal{X} \in \mathbb{R}^{k \times n_e \times n_p}$, maximum number τ of non-zero elements of each fiber of \mathcal{X} , $\eta_1, \eta_2, \eta_3, \eta_X > 1$, $\mu_1, \mu_2, \mu_3, \mu_X > 0$.
 - 2: Set $G_2 \leftarrow (\mathcal{G}_2)_{[2]}$ and $X \leftarrow (\mathcal{X})_{[1]}$
 - 3: Compute $G_1 = P_{\Theta_{n_1, r_1}}(G_1)$, $G_2 = P_{\Theta_{r_1 n_2, r_2}}(G_2)$, $G_3 = P_{\Omega_{r_2, k}}(G_3)$, $X = P_{\Gamma_{k, n_e n_p}^{(\tau)}}(X)$.
 - 4: **repeat**
 - 5: Update G_1 : Set $L'_{G_1} = \max\{\eta_1 L_{G_1}, \mu_1\}$ and $\bar{\alpha}_1 = 1/L'_{G_1}$ and compute $G_1 = P_{\Theta_{n_1, r_1}}(G_1 - \bar{\alpha}_1 \nabla_{G_1} H)$;
 - 6: Update G_2 : Set $L'_{G_2} = \max\{\eta_2 L_{G_2}, \mu_2\}$ and $\bar{\alpha}_2 = 1/L'_{G_2}$ and compute $G_2 = P_{\Theta_{r_1 n_2, r_2}}(G_2 - \bar{\alpha}_2 \nabla_{G_2} H)$;
 - 7: Update G_3 : Set $L'_{G_3} = \max\{\eta_3 L_{G_3}, \mu_3\}$ and $\bar{\alpha}_3 = 1/L'_{G_3}$ and compute $G_3 = P_{\Omega_{r_2, k}}(G_3 - \bar{\alpha}_3 \nabla_{G_3} H)$;
 - 8: Update X : Set $L'_X = \max\{\eta_X L_X, \mu_X\}$ and $\bar{\alpha}_X = 1/L'_X$ and compute $X = P_{\Gamma_{k, n_e n_p}^{(\tau)}}(X - \bar{\alpha}_X \nabla_X H)$;
 - 9: **until** convergence
-

The TT algorithmic version of sPALM can be easily obtained following Algorithms 3 and 2 and replacing the stepsizes $\bar{\alpha}_1, \bar{\alpha}_2, \bar{\alpha}_3$ and $\bar{\alpha}_X$ with the spectral stepsizes based on Algorithm 2 and imposing the Armijo sufficient decrease condition.

REMARK 4. *The same considerations of Proposition 5.1 carry over to the BB stepsizes and the Lipschitz constants for the TT-DL problem (5.5).*

The next theorem contains our main convergence result for PALM-DL-TT described in Algorithm 4. This result can be generalized to *any* PALM-type algorithm applied to the TT DL formulation (5.5).

THEOREM 5.4. *If the sequence generated by PALM-DL-TT in Algorithm 4 is bounded, then it converges to a critical point of the TT formulation of the DL problem (5.5) and it has finite length property.*

Proof. The result is proved by observing that the function H in (5.5) is twice continuously differentiable, the functions in the objective of problem (5.5) are semi-algebraic and satisfy Assumption A. Indeed, all indicator functions are proper, lower semi-continuous and semi-algebraic: the sets $\Omega_{n, m}$ and $\Gamma_{k, n_e n_p}$ are semi-algebraic (see [3, 33]) and $\Theta_{n, m}$ is a closed semi-algebraic set for any n and m . Also, Proposition 5.2 ensures that Assumptions A3-A5 hold (see [10, Remark 3]). \square

6. Numerical experiments. We numerically explore the advantages of using the spectral variant of PALM and the possible benefits of using a TT based algorithm in the solution of the image classification problem. We report experiments using the first classification strategy described in Section 2.1, that is the DL problem is first solved and then the classification matrix W is determined by solving (2.8) The considered algorithms are compared in terms of efficiency and classification performance both in the matrix and tensor settings. A truncated approach for the TT formulation is also tested. Section 6.6 is devoted to the treatment of 5th order tensors, leading to a 4D implementation of our algorithms; numerical experiments on a suitable database are reported, illustrating the effectiveness of the TT approach.

6.1. Description of the databases. We consider four different databases composed of grayscale images with $n = n_1 n_2$ pixels of n_p persons or objects in n_e expressions, where by expression in most cases we mean different illuminations, view angles, etc. Each database can thus be naturally represented as a 4th order tensor $\mathcal{Y} \in \mathbb{R}^{n_1 \times n_2 \times n_e \times n_p}$. The characteristics of all databases are summarized in Table 6.1.

1. MIT-CBCL⁵ [46] is composed by 3240 grayscale images of 10 persons in 324 different expressions. Each image is reduced⁶ to 15×15 pixels.
2. Extended Yale [24] consists of more than 16,000 images of 28 subjects in 585 expressions. Each image is reduced to 20×15 pixels.
3. MNIST [32] contains 28×28 size images of ten handwritten digits (from 0 to 9) split in a training set composed by 60,000 images and a test set composed by 10,000 images. The number of “expressions” for each digit varies. In Table 6.1 the minimum and maximum number of expressions is reported. For our experiments we use 2676 expressions for the training set and 892 for the test set. Notice that the variable expression is not well-defined, i.e., there is no correspondence with two different digits in the j th expression.
4. Fashion-MNIST [48] contains 70,000 images of 10 different kinds of Zalando’s articles; 3,000 images per item for the training set and 1,000 for the test set were used. As for MNIST, the variable “expression” is not well-defined.

Each database of n_p persons in n_e expressions is split into 75% training and 25% test sets, so that $\tilde{n}_e = 0.75n_e$ is the total number of expressions used for training.

Database	pixel size (original)	pixel size (resized)	n_e	n_p
MIT-CBCL	200×200	15×15	324	10
Ext’d Yale shrunk	640×480	20×15	585	28
MNIST	28×28	28×28	[892, 6742]	10
Fashion MNIST	28×28	28×28	7000	10

Table 6.1: Pixel size, number of expressions and persons of all databases.

6.2. Experimental setting. We consider different PALM-type algorithms for the solution of the matrix and tensor DL problems in (2.1) and (2.6), respectively. All the numerical experiments were conducted on one node HPE ProLiant DL560 Gen10 with 4 Intel(R) Xeon(R) Gold 6140 CPU @ 2.30GHz and 100 of the 512 Gb of RAM using Matlab R2019a. We consider the *classification rate* as performance measure, that is, the percentage of correctly classified persons or objects over the total number of test images.

As starting approximations for the tested algorithms, a random dictionary $\mathcal{D} \in \mathbb{R}^{n_1 \times n_2 \times k}$ with unit norm frontal slices and a sparse random tensor $\mathcal{X} \in \mathbb{R}^{k \times n_e \times n_p}$ with at most τ non-zero elements per column fiber were used. Then, for the matrix formulation we set $Y = \mathcal{Y}_{[2]}$, $D = \mathcal{D}_{[2]}$ and $X = \mathcal{X}_{[1]}$. A similar choice is made also for the Tensor-Train setting where G_1 , G_2 and G_3 are initialized as the TT-cores of \mathcal{D} . The parameter k is set such that $n < k < \tilde{n}_e n_p$ as is common in dictionary learning. More precisely, we set $k = 441$ for the face databases, $k = 1225$ for the

⁵Copyright 2003 -2005 Massachusetts Institute of Technology. All Rights Reserved.

⁶To apply the dictionary learning formulation the number of pixels needs to be smaller than the total number of images, that is, $n < n_e n_p$. For this reason a shrunk version of the MIT-CBCL and Extended Yale databases are considered, where the total number of pixels is drastically reduced.

matrix DL problem (2.1)	
PALM-DL	PALM using computation of the exact Lipschitz constant [10]
iPALM-DL	iPALM using computation of the exact Lipschitz constant [40]
iPALMbt-DL	iPALM using backtracking to estimate the Lipschitz constant [40]
sPALM-DL	sPALM based on Algorithms 2-3
TT-DL problem (2.6)	
PALM-DL-TT	PALM using computation of the exact Lipschitz constant as in Algorithm 4
sPALM-DL-TT	sPALM based on Algorithms 2-3

Table 6.2: All methods employed in our experiments.

Fashion MNIST and $k = 1600$ for the MNIST. The sparsity parameter τ depends on the number of classes, n_p , of the database and is set to $4n_p$ for all the databases except MNIST for which $\tau = 2n_p$. Other choices of these parameters have been explored. However, we just report the results for these values of k and τ which seem to exhibit higher classification rate.

We consider the PALM-type algorithms described in Table 6.2. The iPALM algorithm is a variant of PALM, where inertial steps are computed to accelerate convergence [40]. More precisely, given some positive scalars ξ_k^1 and ξ_k^2 , the iterate updates in (3.5) and (3.6) in Algorithm 1 are modified as

$$\begin{aligned}\tilde{x}_k &= x_k + \xi_k^1(x_k - x_{k-1}), \\ x_{k+1} &= \text{prox}_{1/\bar{\alpha}_{k,1}}^{f_1}(\tilde{x}_k - \bar{\alpha}_{k,1}\nabla_x H(\tilde{x}_k, y_k)),\end{aligned}$$

and analogously for the update of the y block using ξ_k^2 . The choice of ξ_k^1 and ξ_k^2 is crucial both for the convergence and the acceleration speed of iPALM; setting $\xi_k^1 = \xi_k^2 = 0$ corresponds to the original PALM. Following the analysis in [40] for the nonconvex case, also the value of η_1 and η_2 should suitably depend on ξ_k^1 and ξ_k^2 , but we found that in practice the choice $\eta_1 = \eta_2 = 1$ yields much better performance. These values have also been adopted for PALM-DL and PALM-DL-TT based on Algorithm 1 while the μ 's are set equal to 10^{-10} . Different values for the ξ_k 's have been tested based on the experience in [40] and we report here results for the best performing ones, that is $\xi_k^1 = \xi_k^2 = 0.2$. The iPALMbt-DL implementation⁷ is a variant of iPALM where the Lipschitz constants are approximated using the backtracking strategy (doubling the attempted values) and decreasing the approximated value if a step yielded sufficient decrease (see also [14]).

Regarding implementations based on the spectral variant in Algorithms 2-3 we set: $\alpha_{\min} = 10^{-10}$, $\alpha_{\max} = 10^{10}$, the initial stepsizes α_0 's are set equal to 1, ρ 's are set equal to 0.5 and δ 's equal to 10^{-4} .

Deriving a reliable criterion for terminating the iteration is a crucial step towards the development of a robust method. Most DL implementations in the literature rely on the number of iterations as stopping criterion. We have also implemented this choice by setting the maximum number of iterations equal to 50 in the forthcoming experiments, where the focus is on discussing the ability of the algorithms in

⁷The implementation of iPALMbt-DL is an adaptation to the DL problem of the code provided by the courtesy of the authors of [40] for the solution of sparse nonnegative factorizations.

classifying images. Nonetheless, we have further investigated the use of a problem-driven stopping criterion in the analysis of the convergence history of the PALM-type algorithms and report the obtained results in Appendix A.

6.3. Preliminary tests on the matrix DL classification problem. In this section we want to explore the potential of the spectral gradient step compared to that based on the Lipschitz constants in the solution of the matrix DL classification problem. To this end we compare sPALM-DL with the original PALM-DL and the inertial variants iPALM-DL and iPALMbt-DL on the four datasets described in Table 6.1.

For the considered methods and all datasets, we report in Table 6.3 the classification performance after 50 iterations and we plot in Figure 6.1 the value of $H(D, X) = \|Y - DX\|_F$ as the CPU time proceed.

Focusing on the existing PALM variants, we observe that PALM-DL, iPALM-DL and iPALMbt-DL reached similar classification performance but iPALMbt-DL is more time consuming. The only exception is in the classification of the MNIST data set for which iPALMbt-DL gains roughly the 10% of classification rate but still at the cost of a higher CPU time (see Figure 6.1). On the other hand sPALM obtains similar percentages for MIT-CBCL and Extended Yale but higher classification performance for the largest data sets, i.e. MNIST and Fashion MNIST, and being in fact the fastest PALM variant.

	PALM-DL	iPALM-DL	iPALMbt-DL	sPALM-DL
MIT-CBCL	100%	100%	100%	100%
Ext'd Yale shrunk	93.7%	93.8%	94.2%	93.4%
MNIST	64.6%	65.3%	76.6%	80.4%
Fashion MNIST	70.0%	70.7%	71.6%	74.3%

Table 6.3: Successful classification rates of PALM-DL, iPALM-DL, iPALMbt-DL, sPALM-DL on four different databases.

For the sake of completeness we also report in Table 6.4 a comparison between the classical K-SVD method [1]⁸ and the sPALM-DL algorithm in terms of CPU time needed to obtain a comparable value of the objective function. For this experiment, sPALM was run until the objective function value was smaller than that of the objective function obtained with two iterations of K-SVD. Notice that for all the databases, except MNIST, sPALM-DL takes less CPU time than K-SVD, although K-SVD uses optimized MEX functions written in C. Focusing on MNIST, we observe that sPALM takes 84.7 seconds to reach the value of the residual obtained by K-SVD within the 5%.

6.4. Matrix vs tensor DL classification problem. Given the training set $\mathcal{Y} \in \mathbb{R}^{n_1 \times n_2 \times \tilde{n}_e \times n_p}$, we now solve the DL classification problem using either a matrix or a tensor formulation. The matrix DL problem (5.1) is solved using PALM-DL and sPALM-DL. The tensor problem (5.5) is solved by PALM-DL-TT and sPALM-DL-TT. In all cases, the classification matrix W is then computed by solving (2.8).

Figure 6.2 displays the classification success rate of all algorithms as the iterations proceed. The use of a spectral step results in higher classification performance for all

⁸We used the Matlab implementation KSVD-Box v13 of K-SVD available at <http://www.cs.technion.ac.il/~ronrubin/software.html>

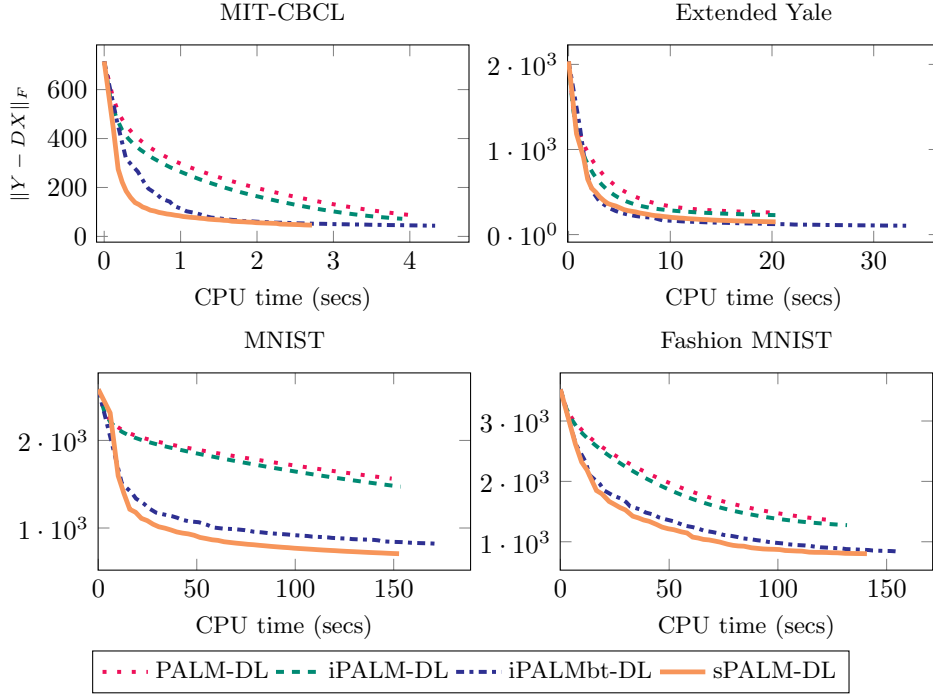


Fig. 6.1: Residual norm history for PALM-DL, iPALM-DL, iPALMbt-DL, sPALM-DL (50 iterations).

	sPALM-DL		K-SVD	
	$\ Y - DX\ _F$	CPU time	$\ Y - DX\ _F$	CPU time
MIT-CBCL	61.9	1.7	62.7	8.6
Ext'd Yale shrunk	109.7	77.7	109.8	148.3
MNIST	761.1	105.4	763.1	91.3
Fashion MNIST	827.7	114.4	829.5	140.9

Table 6.4: Value of the objective function and CPU time memory requirements for sPALM-DL and K-SVD.

examined data. For the MIT-CBCL, sPALM based algorithms achieve the maximum classification rate after 20 iterations while PALM-DL and PALM-DL-TT need more iterations to reach the same rate. When processing MNIST the classification performance of PALM-DL and PALM-DL-TT decreases as iterations progress, suggesting overfitting, whereas a slight improvement occurs with sPALM-DL and sPALM-DL-TT. On these datasets, the Tensor-Train formulation does not seem to be beneficial for classification purposes. Computer memory limitations however may favour the tensor approach, as we will discuss in the next section.

6.5. Memory saving truncated approach. One of the challenges in dealing with huge databases is to reduce memory requirements. For a database $\mathcal{Y} \in$

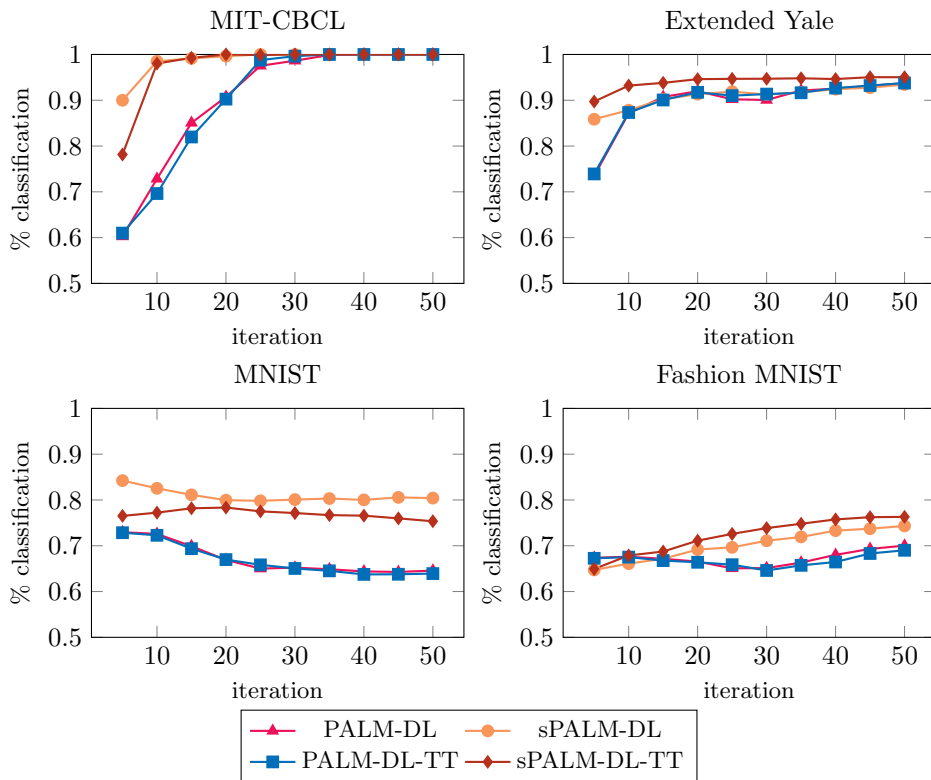


Fig. 6.2: Classification performance of PALM-DL, sPALM-DL, PALM-DL-TT and sPALM-DL-TT with respect to the number of iterations for four different database, using the formulations of Section 2.

$\mathbb{R}^{n_1 \times n_2 \times n_e \times n_p}$, PALM-DL and sPALM-DL store $\mathcal{D} \in \mathbb{R}^{n_1 \times n_2 \times k}$ and (sparse) $\mathcal{X} \in \mathbb{R}^{k \times n_e \times n_p}$, requiring $m_P := n_1 n_2 k + \tau n_e n_p$ memory allocations. This quantity can be quite large in real image applications. We next investigate the possibility of truncating the tensor decomposition, possibly without interfering with the classification performance. In the Tensor-Train based algorithms PALM-DL-TT and sPALM-DL-TT storage for the arrays $G_1 \in \mathbb{R}^{n_1 \times r_1}$, $G_2 \in \mathbb{R}^{r_1 \times n_2 \times r_2}$, $G_3 \in \mathbb{R}^{r_2 \times k}$ and $\mathcal{X} \in \mathbb{R}^{k \times n_e \times n_p}$ is required, yielding $m_{TT} := n_1 r_1 + r_1 n_2 r_2 + r_2 k + \tau n_e n_p$ allocations. The value of r_2 determines whether the (truncated) TT approach is more memory efficient than the full scheme by comparing m_{TT} and m_P . In Figure 6.3 we show the classification rates for all TT based methods on two of the datasets after 50 iterations, as r_2 varies up to the maximum value obtainable for that dataset ($r_2 \leq 225$ and $r_2 \leq 300$ for MIT-CBCL and Extended Yale, resp.). We note that the TT variants are able to achieve good classification performance also with small values of r_2 . In particular, for the MIT-CBCL and sPALM-DL-TT choosing a value of r_2 greater than 40 has no benefit on the classification performance, suggesting the use of $r_2 = 40$, thus reducing the overall memory costs with respect to PALM ($m_P = 108,945$ vs $m_{TT} = 36,585$). Similarly, for Extended Yale the value $r_2 = 150$ can be chosen without dramatically spoiling the classification performance. In other words the Tensor-Train Decomposition enables us to store the information for classification purposes in a more compact

manner.

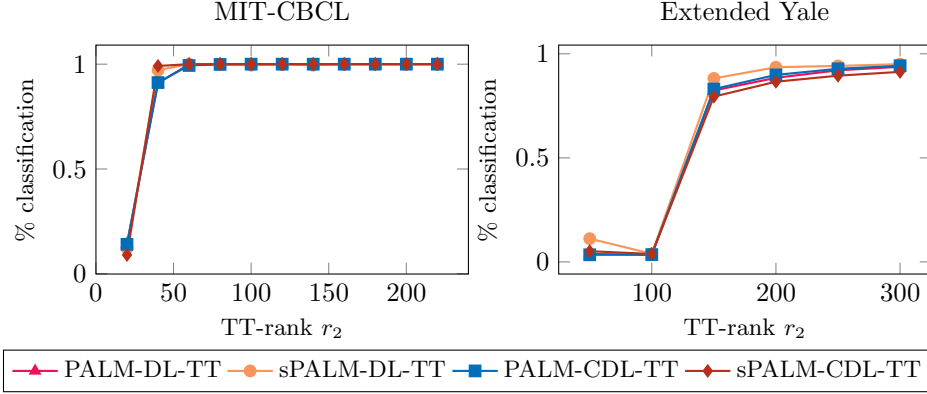


Fig. 6.3: Classification performance of the Tensor-Train based algorithms for different values of the TT-rank r_2 .

6.6. A classification example in 4D setting. The Tensor-Train decomposition allows us to readily extend the 3D formulation, explored in the previous sections, to higher-order tensors. In the following we analyze the classification performance of PALM-DL-TT and sPALM-DL-TT for a 5th order tensor $\mathcal{Y} \in \mathbb{R}^{n_1 \times n_2 \times n_3 \times \tilde{n}_e \times n_p}$ and we compare them with their matrix versions PALM-DL and sPALM-DL. First of all, we write the TT dictionary learning problem as in (2.7) with $q = 3$ and $s = 5$. Furthermore, we notice that

$$\|\mathcal{Y} - (G_1 \times_{\frac{1}{2}} G_2 \times_{\frac{1}{3}} G_3 \times_{\frac{1}{3}} G_4) \times_{\frac{1}{4}} \mathcal{X}\|_F = \|\mathcal{Y}_{[3]} - (I_{n_2 n_3} \otimes G_1) (I_{n_3} \otimes (G_2)_{[2]}) (G_3)_{[2]} G_4 \mathcal{X}_{[1]}\|_F \quad (6.1)$$

where $G_1, (G_2)_{[2]}, (G_3)_{[2]}$, are matrices with orthonormal columns, and more precisely, $G_1 \in \Theta_{n_1, r_1}$, $(G_2)_{[2]} \in \Theta_{r_1 n_2, r_2}$, $(G_3)_{[2]} \in \Theta_{r_2 n_3, r_3}$ while $G_4 \in \Omega_{r_3, k}$ has unit norm columns. The following proposition provides an expression for the gradient of H and corresponding Lipschitz constants using the orthogonality of the first three TT-cores.

PROPOSITION 6.1. *Let $G_2 = (G_2)_{[2]}$, $G_3 = (G_3)_{[2]}$, $X = \mathcal{X}_{[1]}$, $Y = \mathcal{Y}_{[3]}$ and*

$$H(G_1, G_2, G_3, G_4, X) = \|Y - (I_{n_2 n_3} \otimes G_1) (I_{n_3} \otimes G_2) G_3 G_4 X\|_F^2.$$

Then the partial gradients of H satisfy Assumption A3. Moreover, the following upper bounds for the Lipschitz constants hold: $L_X = 2\|G_4\|_2^2$, $L_{G_3} = 2\|G_4 X\|_2^2$, $L_{G_4} = 2\|X\|_2^2$, $L_{G_1} = 2\|\sum_{i=1}^p A_i A_i^T\|_2$, $L_{G_2} = 2\|\sum_{i=1}^p B_i B_i^T\|_2$, where $A_i \in \mathbb{R}^{r_1 \times n_2}$ is the matricization of the i th column of $A = (I_{n_3} \otimes G_2) G_3 G_4 X$ and $B_i \in \mathbb{R}^{r_1 \times n_2}$ is the matricization of the i th column of $B = G_3 G_4 X$.

Proof. By direct computation we obtain the following expressions for the partial gradients of H :

$$\nabla_X H = -2(I_{n_2 n_3} \otimes G_1) (I_{n_3} \otimes G_2) G_3 G_4^T Y + 2(G_3 G_4)^T G_3 G_4 X$$

and $\nabla_{G_1} H = 2\sum_{i=1}^p (-Y_i + G_1 A_i) A_i^T$, where Y_i denotes the matricization of the i th column of Y , $\nabla_{G_2} H = 2\sum_{i=1}^p (-Y_i + G_1 B_i) B_i^T$,

$$\nabla_{G_3} H = 2((I_{n_2 n_3} \otimes G_1) (I_{n_3} \otimes G_2))^T (-Y + (I_{n_2 n_3} \otimes G_1) (I_{n_3} \otimes G_2) G_3 G_4 X) (G_4 X)^T.$$

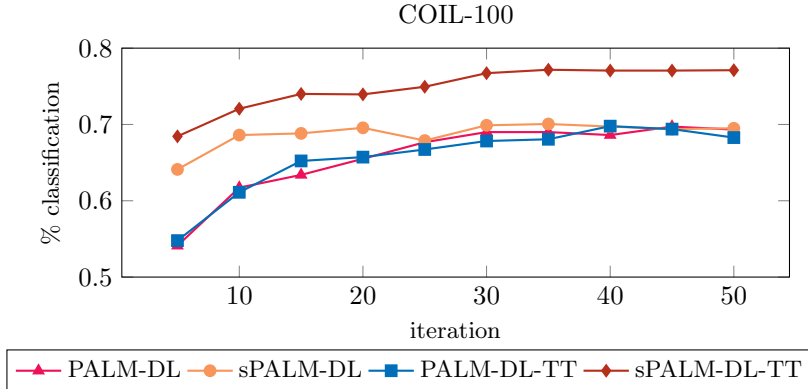


Fig. 6.4: Classification performance of PALM-DL, sPALM-DL, PALM-DL-TT and sPALM-DL-TT with respect to the number of iterations for the COIL-100 database.

For ∇_{G_4} , we have $\nabla_{G_4} H = 2C^T(-Y + CG_4X)X^T$, where $C = (I_{n_2n_3} \otimes G_1)(I_{n_3} \otimes G_2)G_3$. Using these expressions we follow the proof of Proposition 5.2 to obtain the required Lipschitz moduli. \square

To test this formulation we consider the COIL-100 database [37], containing RGB images of $n_p = 100$ different objects in $n_e = 72$ view angles. For this experiment the size of each image is reduced to $16 \times 16 \times 3$ to preserve the relation among the number of pixels $n = n_1n_2n_3$, the atoms of the dictionary k and the total number of images n_en_p (i.e., $n < k < n_en_p$). The training set \mathcal{Y} is composed by all the objects in $\tilde{n}_e = 54$ different view angles, corresponding to 75% of the total number of images. We set the number of atoms to $k = 1400$ and the sparsity parameter to $\tau = 4n_p$. The reported results correspond to the classification success along the iterations for a maximum of 50 iterations. From Figure 6.4 we can notice that the spectral step enhances the classification rate significantly for the TT formulation. In particular at the 50th iteration the classification rate of sPALM-DL-TT is equal to 77.11% while the other methods do not reach 70%. Furthermore we observe that using a number of iterations greater than 30 has almost no impact on the classification rate.

7. Conclusions. Exploiting data multidimensionality is crucial in dictionary learning and, in particular, when DL is applied to image classification. To address this challenge, we have devised the new method sPALM in the class of PALM-type convergent algorithms, and proposed both a matrix and tensor-train formulation for its implementation. The new approach implicitly includes second order information by using spectral stepsizes that exploit the alternating iteration history. The resulting algorithm is competitive with respect to different recent variants of PALM, as illustrated by our numerical experiments. Moreover, since sPALM is described for general nonconvex non-smooth problems, it may serve as a basis for further algorithmic acceleration techniques [12, 28, 40]. Finally, we have experimentally shown that the TT formulation may bring advantages in terms of memory requirements and rate of successful classification, especially when applied to 4D databases.

Acknowledgments. We would like to thank Nicolas Gillis for insightful comments on a previous version of this work.

Data availability. The data that support the findings of this study are available from the corresponding author upon request.

REFERENCES

- [1] M. AHARON, M. ELAD, AND A. BRUCKSTEIN, *K-SVD: An algorithm for designing overcomplete dictionaries for sparse representation*, IEEE Trans. on Signal Processing, 54 (2006), pp. 4311–4322.
- [2] H. ATTOUCH, J. BOLTE, P. REDONT, AND A. SOUBEYRAN, *Proximal alternating minimization and projection methods for nonconvex problems: An approach based on the Kurdyka-Lojasiewicz inequality*, Mathematics of Operations Research, 35 (2010), pp. 438–457.
- [3] C. BAO, H. JI, Y. QUAN, AND Z. SHEN, *L_0 norm based dictionary learning by proximal methods with global convergence*, in 2014 IEEE Conference on Computer Vision and Pattern Recognition, CVPR 2014, Columbus, OH, USA, June 23–28, 2014, IEEE Computer Society, 2014, pp. 3858–3865.
- [4] J. BARZILAI AND J. M. BORWEIN, *Two-Point Step Size Gradient Methods*, IMA J. Numer. Anal., 8 (1988), pp. 141–148.
- [5] H. H. BAUSCHKE AND P. L. COMBETTES, *Convex analysis and monotone operator theory in Hilbert spaces*, vol. 408, Springer, 2011.
- [6] A. BECK, *First-order methods in optimization*, SIAM, 2017.
- [7] A. BECK AND M. TEBoulLE, *A fast iterative shrinkage-thresholding algorithm for linear inverse problems*, SIAM J. Imaging Sci., 2 (2009), pp. 183–202.
- [8] E. G. BIRGIN, J. M. MARTÍNEZ, AND M. RAYDAN, *Nonmonotone spectral projected gradient methods on convex sets*, SIAM J. Optim., 10 (2000), pp. 1196–1211.
- [9] E. G. BIRGIN, J. M. MARTÍNEZ, AND M. RAYDAN, *Spectral projected gradient methods: review and perspectives*, Journal of Statistical Software, 60 (2014), pp. 1–21.
- [10] J. BOLTE, S. SABACH, AND M. TEBoulLE, *Proximal alternating linearized minimization for nonconvex and nonsmooth problems*, Math. Program., 146 (2014), pp. 459–494.
- [11] S. BONETTINI, *Inexact block coordinate descent methods with application to non-negative matrix factorization*, IMA J. Numer. Anal., 31 (2011), pp. 1431–1452.
- [12] S. BONETTINI, I. LORIS, F. PORTA, AND M. PRATO, *Variable metric inexact line-search-based methods for nonsmooth optimization*, SIAM J. Optim., 26 (2016), pp. 891–921.
- [13] D. BRANDONI, *Tensor-Train decomposition for image classification problems*, PhD thesis, University of Bologna, 2022.
- [14] L. BUNGERT, D. A. COOMES, M. J. EHRHARDT, J. RASCH, R. REISENHOFER, AND C.-B. SCHÖNLIEB, *Blind image fusion for hyperspectral imaging with the directional total variation*, Inverse Problems, 34 (2018), p. 044003.
- [15] A. CICHOCKI, *Era of big data processing: A new approach via tensor networks and tensor decompositions*, CoRR, abs/1403.2048 (2014).
- [16] C. F. DANTAS, J. E. COHEN, AND R. GRIBONVAL, *Learning tensor-structured dictionaries with application to hyperspectral image denoising*, in 27th European Signal Processing Conference, EUSIPCO 2019, A Coruña, Spain, September 2–6, 2019, IEEE, 2019, pp. 1–5.
- [17] D. DAVIS, M. UDELL, AND B. EDMUNDS, *The sound of APALM clapping: Faster nonsmooth nonconvex optimization with stochastic asynchronous palm*, in Proceedings of the 30th International Conference on Neural Information Processing Systems, NIPS’16, Red Hook, NY, USA, 2016, Curran Associates Inc., p. 226–234.
- [18] D. DI SERAFINO, V. RUGGIERO, G. TORALDO, AND L. ZANNI, *On the steplength selection in gradient methods for unconstrained optimization*, Applied Mathematics and Computation, 318 (2018), pp. 176–195.
- [19] G. DUAN, H. WANG, Z. LIU, J. DENG, AND Y. CHEN, *K-CPD: learning of overcomplete dictionaries for tensor sparse coding*, in Proceedings of the 21st International Conference on Pattern Recognition, ICPR 2012, Tsukuba, Japan, November 11–15, 2012, IEEE Computer Society, 2012, pp. 493–496.
- [20] B. DUMITRESCU AND P. IROFTI, *Dictionary learning algorithms and applications*, Springer, 2018.
- [21] K. ENGAN, S.O. AASE, AND J. HAKON HUSOY, *Method of optimal directions for frame design*, in 1999 IEEE International Conference on Acoustics, Speech, and Signal Processing. Proceedings. ICASSP99 (Cat. No.99CH36258), vol. 5, 1999, pp. 2443–2446.
- [22] J. FAN, C. YANG, AND M. UDELL, *Robust non-linear matrix factorization for dictionary learning, denoising, and clustering*, IEEE Trans. on Signal Processing, 69 (2021), pp. 1755–1770.
- [23] X. GAO, X. CAI, AND D. HAN, *A Gauss-Seidel type inertial proximal alternating linearized*

- minimization for a class of nonconvex optimization problems*, J. Glob. Optim., 76 (2020), pp. 863–887.
- [24] A.S. GEORGHIADES, P.N. BELHUMEUR, AND D.J. KRIEGMAN, *From few to many: Illumination cone models for face recognition under variable lighting and pose*, IEEE Trans. Pattern Anal. Mach. Intelligence, 23 (2001), pp. 643–660.
- [25] M. GHASSEMI, Z. SHAKERI, A. D. SARWATE, AND W. U. BAJWA, *Learning mixtures of separable dictionaries for tensor data: Analysis and algorithms*, IEEE Transactions on Signal Processing, 68 (2019), pp. 33–48.
- [26] L. GRIPPO AND M. SCIANDRONE, *On the convergence of the block nonlinear Gauss-Seidel method under convex constraints*, Operations Research Letters, 26 (2000), pp. 127–136.
- [27] L. GRIPPO AND M. SCIANDRONE, *Nonmonotone derivative-free methods for nonlinear equations*, Comput. Optim. Appl., 37 (2007), pp. 297–328.
- [28] L.T.K. HIEN, D.N. PHAN, AND N. GILLIS, *An inertial block majorization minimization framework for nonsmooth nonconvex optimization*, arXiv preprint arXiv:2010.12133, (2020).
- [29] B. IANNAZZO AND M. PORCELLI, *The Riemannian Barzilai–Borwein method with nonmonotone line search and the matrix geometric mean computation*, IMA J. Numer. Anal., 38 (2018), pp. 495–517.
- [30] CH. KANZOW AND TH. LECHNER, *Globalized inexact proximal newton-type methods for nonconvex composite functions*, Comput. Optim. Appl., 78 (2021), pp. 377–410.
- [31] T.G. KOLDA AND B. W. BADER, *Tensor decompositions and applications*, SIAM review, 51 (2009), pp. 455–500.
- [32] Y. LECUN, L. BOTTOU, Y. BENGIO, AND P. HAFFNER, *Gradient-based learning applied to document recognition*, Proceedings of the IEEE, 86 (1998), pp. 2278–2324.
- [33] Z. LI, S. DING, W. CHEN, Z. YANG, AND S. XIE, *Proximal alternating minimization for analysis dictionary learning and convergence analysis*, IEEE Trans. on Emerging Topics in Computational Intelligence, 2 (2018), pp. 439–449.
- [34] J. MAIRAL, F.R. BACH, AND J. PONCE, *Sparse modeling for image and vision processing*, Found. Trends. Comput. Graph. Vis., 8 (2014), pp. 85–283.
- [35] E. MELI, B. MORINI, M. PORCELLI, AND C. SGATTONI, *Solving nonlinear systems of equations via spectral residual methods: stepsize selection and applications*, Journal of Scientific Computing, 90 (2022), pp. 1–41.
- [36] B. S. MORDUKHOVICH, *Variational analysis and generalized differentiation I: Basic theory*, vol. 330, Springer Science & Business Media, 2006.
- [37] S. A. NENE, S. K. NAYAR, AND H. MURASE, *Columbia Object Image Library (COIL-100)*, Tech. Report CUCS-006-96, Department of Computer Science, Columbia University, Feb 1996.
- [38] B. A. OLSHAUSEN AND D. J. FIELD, *Sparse coding with an overcomplete basis set: A strategy employed by V1?*, Vision research, 37 (1997), pp. 3311–3325.
- [39] I.V. OSELEDETS, *Tensor-train decomposition*, SIAM J. Sci. Comput., 33 (2011), pp. 2295–2317.
- [40] T. POCK AND S. SABACH, *Proximal alternating linearized minimization (iPALM) for nonconvex and nonsmooth problems*, SIAM J. Imaging Sci., 9 (2016), pp. 1756–1787.
- [41] F. ROEMER, G. DEL GALDO, AND M. HAARDT, *Tensor-based algorithms for learning multidimensional separable dictionaries*, in 2014 IEEE International Conference on Acoustics, Speech and Signal Processing (ICASSP), 2014, pp. 3963–3967.
- [42] R. RUBINSTEIN, A. M. BRUCKSTEIN, AND M. ELAD, *Dictionaries for sparse representation modeling*, Proceedings of the IEEE, 98 (2010), pp. 1045–1057.
- [43] R. RUBINSTEIN, M. ZIBULEVSKY, AND M. ELAD, *Efficient implementation of the K-SVD algorithm using batch orthogonal matching pursuit*, Tech. Report CS-2008-08, Computer Science Department, Technion, 2008.
- [44] Z. SHAKERI, A. D. SARWATE, AND W. U. BAJWA, *Identifiability of kronecker-structured dictionaries for tensor data*, IEEE Journal of Selected Topics in Signal Processing, 12 (2018), pp. 1047–1062.
- [45] E. P. SIMONCELLI, W. T. FREEMAN, E. H. ADELSON, AND D. J. HEEGER, *Shiftable multiscale transforms*, IEEE Transactions on Information Theory, 38 (1992), pp. 587–607.
- [46] B. WEYRAUCH, B. HEISELE, J. HUANG, AND V. BLANZ, *Component-based face recognition with 3D morphable models*, in 2004 Conference on Computer Vision and Pattern Recognition Workshop, 2004, pp. 85–85.
- [47] S. J. WRIGHT, R. D. NOWAK, AND M. A. T. FIGUEIREDO, *Sparse reconstruction by separable approximation*, IEEE Trans. on signal processing, 57 (2009), pp. 2479–2493.
- [48] H. XIAO, K. RASUL, AND R. VOLLGRAF, *Fashion-MNIST: a novel image dataset for benchmarking machine learning algorithms*, arXiv preprint arXiv:1708.07747, (2017).
- [49] Z. ZHANG AND S. AERON, *Denoising and completion of 3D data via multidimensional dictionary learning*, arXiv preprint arXiv:1512.09227v1, (2015).

- [50] H. ZHU AND M.K. NG, *Structured dictionary learning for image denoising under mixed gaussian and impulse noise*, IEEE Trans. Image Process., 29 (2020), pp. 6680–6693.
- [51] S. ZUBAIR AND W. WANG, *Tensor dictionary learning with sparse tucker decomposition*, in 2013 18th International Conference on Digital Signal Processing (DSP), 2013, pp. 1–6.

Appendix A. Analysis of the convergence history of the PALM variants in solving the DL problem. In this section we compare the matrix based methods in Table 6.2 for the solution of the matrix DL problem (2.1). To this purpose, in addition to a safeguard strategy on a maximum (loose) number of iterations, we consider the following stopping criterion based on iterate variation, that takes into account possible different scalings in the block variables. The criterion is given by $\|\bar{D} - D\|_F \leq \text{tol}_D$, $\|\bar{X} - X\|_F \leq \text{tol}_X$. Here the upper bar denotes the approximate solution from the previous iteration and tol_D and tol_X are tolerances set equal to $\text{tol}_D = 10^{-3} \sqrt{n_1 n_2 k}$ and $\text{tol}_X = 10^{-3} \sqrt{k n_e n_p}$.

The plots in Figure A.1 show the values of $H(D, X) = \|Y - DX\|_F$ as the CPU time proceeds, for the datasets in Table 6.1. As expected, the use of a backtracking rule (iPALMbt-DL) to estimate the Lipschitz constants yields a much faster decrease in the residual value than using the constant stepsize (PALM-DL and iPALM-DL) but each iteration of iPALMbt-DL is more expensive, see the steeper slope in Figure A.2. Moreover, for all the databases, sPALM-DL converges in far fewer iterations than iPALMbt-DL, resulting in a significantly lower overall CPU time than for the other methods. These results illustrate the advantage of using higher order information.

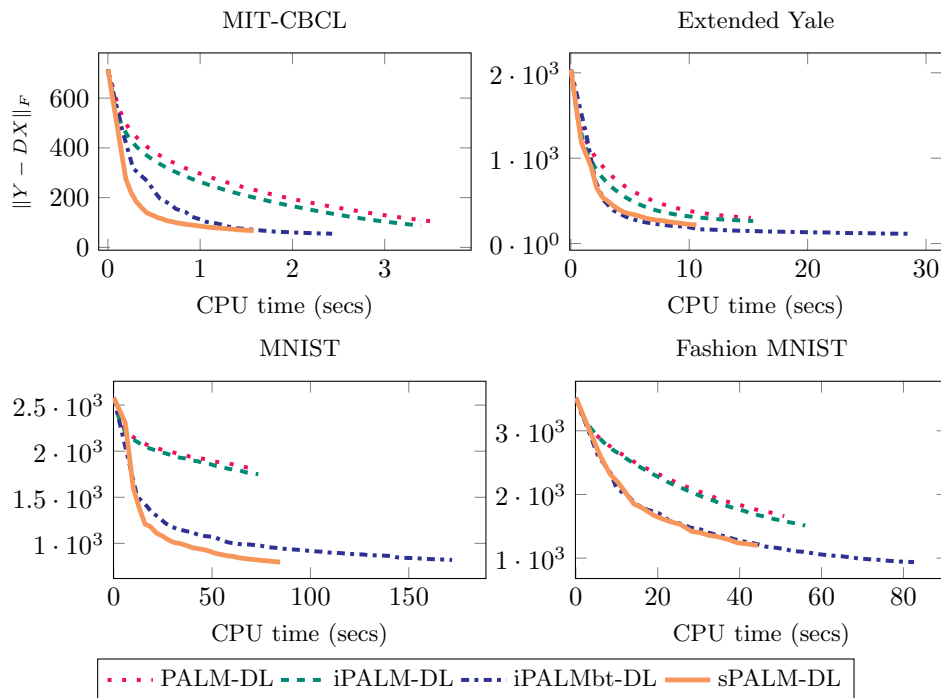


Fig. A.1: Residual norm history for PALM-DL, iPALM-DL, iPALMbt-DL, sPALM-DL.

Appendix B. Tools for Tensor-Train Decomposition. In this section we

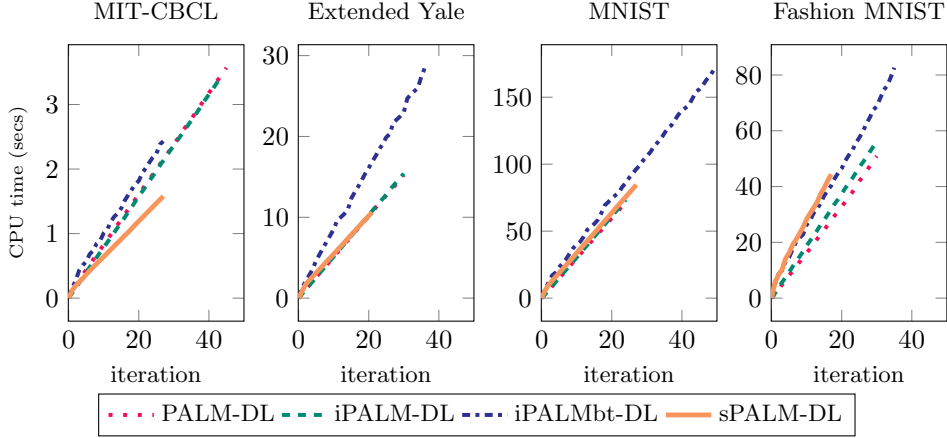


Fig. A.2: CPU time as iterations increase, for PALM-DL, iPALM-DL, iPALMbt-DL, sPALM-DL.

introduce some tensor notation and useful tools. The *fibers* of a tensor are obtained by fixing every index but one. In particular for third order tensors we can define column fibers (last two indices fixed), row fibers (first and third indices fixed) and tube fibers (first two indices fixed). The *slices* of a tensor are defined by fixing only one index. For third order tensors, we can define the horizontal slices (first index fixed), the lateral slices (second index fixed) and the frontal slices (third index fixed).

DEFINITION B.1. [31, p. 458] Given two tensors $\mathcal{A} \in \mathbb{R}^{I_1 \times \dots \times I_N}$ and $\mathcal{B} \in \mathbb{R}^{I_1 \times \dots \times I_N}$, the scalar product between \mathcal{A} and \mathcal{B} is defined as

$$\langle \mathcal{A}, \mathcal{B} \rangle = \sum_{i_N=1}^{I_N} \dots \sum_{i_1=1}^{I_1} a_{i_1, \dots, i_N} b_{i_1, \dots, i_N}. \quad (\text{B.1})$$

The Frobenius norm of a tensor is given by $\|\mathcal{A}\|_F^2 = \langle \mathcal{A}, \mathcal{A} \rangle$. If \mathcal{A} and \mathcal{B} are matrices, i.e. second order tensors, (B.1) reduces to the standard definition of matrix scalar product. We next define a tensor-matrix multiplication (i.e. *n-mode product*) and a tensor-tensor multiplication (i.e. $\binom{m}{n}$ *mode product*).

DEFINITION B.2. [31, p. 460] Let $\mathcal{A} \in \mathbb{R}^{I_1 \times I_2 \times \dots \times I_N}$ and $U \in \mathbb{R}^{J \times I_n}$. The *n-mode product* $\mathcal{A} \times_n U \in \mathbb{R}^{I_1 \times \dots \times I_{n-1} \times J \times I_{n+1} \times \dots \times I_N}$ is given by

$$(\mathcal{A} \times_n U)_{i_1, \dots, i_{n-1}, j, i_{n+1}, \dots, i_N} = \sum_{i_n=1}^{I_n} a_{i_1, i_2, \dots, i_n, \dots, i_N} u_{j, i_n}$$

The *n-mode product* satisfies the commutative property when the multiplications are performed along different modes.

DEFINITION B.3. [15] The $\binom{m}{n}$ -*product* of a tensor $\mathcal{A} \in \mathbb{R}^{I_1 \times I_2 \times \dots \times I_N}$ with a tensor $\mathcal{B} \in \mathbb{R}^{J_1 \times J_2 \times \dots \times J_M}$, such that $I_n = J_m$, is defined as $\mathcal{C} = \mathcal{A} \times_n^m \mathcal{B}$, where $\mathcal{C} \in \mathbb{R}^{I_1 \times \dots \times I_{n-1} \times I_{n+1} \times \dots \times I_N \times J_1 \times \dots \times J_{m-1} \times J_{m+1} \times \dots \times J_M}$. Its entries are given by

$$\mathcal{C}(i_1, \dots, i_{n-1}, i_{n+1}, \dots, i_N, j_1, \dots, j_{m-1}, j_{m+1}, \dots, j_M) = \sum_{i_n=1}^{I_n} \mathcal{A}(i_1, \dots, i_{n-1}, i_n, i_{n+1}, \dots, i_N) \mathcal{B}(j_1, \dots, j_{m-1}, i_n, j_{m+1}, \dots, j_M).$$

Finally we define the *unfolding* or matricization, i.e. the process of flattening a tensor into a matrix. There are several ways to define it, and we consider the one used by Oseledets in [39]. Let $\mathcal{A} \in \mathbb{R}^{I_1 \times I_2 \times \dots \times I_N}$, then the k th unfolding of \mathcal{A} is the matrix $A_{[k]} \in \mathbb{R}^{(I_1 I_2 \dots I_k) \times (I_{k+1} I_{k+2} \dots I_N)}$, with elements

$$A_{[k]}(\overline{i_1 \dots i_k}, \overline{i_{k+1} \dots i_N}) = \mathcal{A}(i_1, \dots, i_k, i_{k+1}, \dots, i_N), \quad (\text{B.2})$$

where $\overline{i_1 \dots i_N} = i_1 + (i_2 - 1)I_1 + \dots + (i_N - 1)I_1 \dots I_{N-1}$.

We can thus define the *Tensor-Train* decomposition of an N -way array into a product of third order tensors, called TT-cores.

DEFINITION B.4. *Given an N th order tensor \mathcal{A} , its Tensor-Train Decomposition is given by the following*

$$\begin{aligned} \mathcal{A}(i_1, \dots, i_N) &= G_1(i_1, :) \mathcal{G}_2(:, i_2, :) \mathcal{G}_3(:, i_3, :) \dots G_N(i_N, :) \\ &= G_1(i_1) \mathcal{G}_2(i_2) \mathcal{G}_3(i_3) \dots G_N(i_N) \end{aligned} \quad (\text{B.3})$$

Using Definition B.3 for the $\binom{m}{n}$ -mode product, (B.3) can be written as

$$\mathcal{A} = G_1 \times_2^1 \mathcal{G}_2 \times_3^1 \mathcal{G}_3 \times_3^1 \dots \times_3^1 G_N. \quad (\text{B.4})$$

If \mathcal{A} is a third-order tensor then the Tensor-Train Decomposition reduces to the Tucker decomposition, $\mathcal{A} = \mathcal{G}_2 \times_1 G_1 \times_3 G_3^T$. Finally, for general N th order tensor, the Tensor-Train algorithm requires that the matrices $(\mathcal{G}_i)_{[2]}$, $i = 1, \dots, N - 1$ have orthonormal columns.